I&EC research
Industrial & Engineering Chemistry Research

pubs.acs.org/IECR

Article

Optimal Design and Operation of Solid Sorbent Direct Air Capture Processes at Varying Ambient Conditions

Jan F. Wiegner, Alexa Grimm, Lukas Weimann, and Matteo Gazzani*

Cite This: *Ind. Eng. Chem. Res.* 2022, 61, 12649−12667

Read Online

ACCESS | Metrics & More | Article Recommendations | Supporting Information

ABSTRACT: The economic, environmental, and energetic performance of direct air capture (DAC) processes based on solid sorbents depends significantly on ambient air conditions and the availability of renewable resources. High ambient temperature or low humidity leads to higher energy consumption and lower CO_2 productivity; lack of renewable resources may make the direct air capture process not viable. With this work, we investigated how the performance of sorbent-based direct air capture plants varies when changing ambient conditions and how the system should be optimally designed and operated to match the time-dependent variations. To this end, we formulated a new modeling framework, where thermodynamic modeling of adsorption processes is bridged to mixed integer linear optimization via a portable linear model of DAC. The process is based on a vacuum-temperature swing cycle, whose performance was obtained with a rate-based thermodynamic model at varying ambient conditions for an exemplary sorbent representative of different amine-functionalized materials. The optimal design and operation were investigated for (i) a stand-alone DAC system installed at three different geographical locations and (ii) a DAC system embedded in a multi-energy hub aimed at supplying the DAC energy demand from renewable resources. We found that DAC performance is optimal when the process can adjust the operating variables according to the weather profile and when CO_2 can be produced flexibly over time, for example, by adopting a buffer storage tank. Other operation strategies are suboptimal but might require less sophisticated control systems. Moreover, the results suggest that capturing costs are significantly smaller in cold and humid conditions. This conclusion holds for both the stand-alone and the integrated DAC systems. However, for the latter, cold and humid conditions are favorable only when abundant renewable energy is available and can be supplied at low costs, for example, via wind farms. These conclusions remain true over a wide range of technical and cost assumptions.

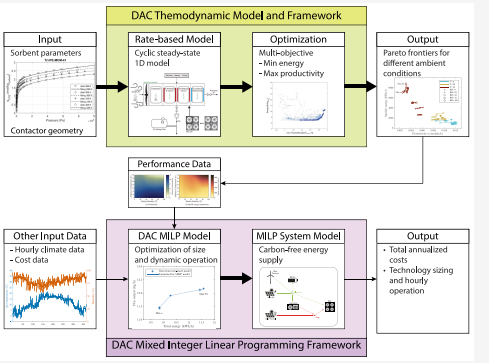

1. INTRODUCTION

Carbon dioxide removal (CDR) technologies, where CO_2 is removed from the atmosphere for permanent storage, are pivotal to keep the global temperature increase below 1.5 °C.[1,2] Notably, CDR provides a solution to compensate emissions from sources that are too difficult (technically or economically) to decarbonize such as air transport, the chemical industry and agriculture.[3−5] Unfortunately, the set of feasible CDR technologies is limited. Minx et al.[6] provide an excellent overview starting from two respective capturing mechanisms and evaluate them for their suitability. The first set of technologies, namely plant-based solutions, bind CO_2 in biomass via photosynthesis. They include reforestation and biomass with carbon capture and storage. The second set of options take advantage of artificial processes for CO_2 removal. DAC is a prominent example of such a process that employs materials and processes that absorb CO_2 from ambient conditions and release it at high concentrations (+95%vol). Compared to plant-based solutions, it has the advantage of lower area requirements, a large capture potential and smaller side effects for biodiversity and food production.[6,7] However, it consumes large amounts of energy, which must be provided as heat, electricity, or chemical energy. While being commercial, DAC processes are still at an early stage of development and suffer from high up-front investment costs.[1,8] The high investment costs and the energy requirements are in fact the main barriers for a large-scale deployment of DAC.

Two main DAC technology pathways exist, which depend on the material binding the CO_2: (1) *aqueous solvent processes* bind CO_2 in liquids and recover it from the solvent via heat or electricity supply. The CO_2 reacts with the liquid solvent in a packed bed air contactor (a column or an engineered contactor for DAC[9]) and is released in a regeneration step that may consist of a stripper, a more sophisticated ensemble of chemical reactors, or an electrochemical device.[9,10] (2) *Solid sorbent processes* adsorb CO_2 on the surface of a solid material and

Received: February 28, 2022
Revised: May 28, 2022
Accepted: July 25, 2022
Published: August 9, 2022

Table 1. Studies on the Effect of Temperature and Humidity on the Performance of Sorbent Materials

material	humidity		temperature		source
	capacity	energy	capacity	energy	
Nanofibrillated cellulose framework coated with PEI	increase	na	na	na	Sehaqui et al.[25]
Fumed silica with PEI coating	ambiguous	na	na	na	Goeppert et al.[21]
Amine-functionalized cellulose	increase	increase	decrease	na	Gebald et al.[35]
Amine-functionalized cellulose	increase	increase	decrease	na	Wurzbacher et al.[27]
Amine-functionalized cellulose	increase	increase	decrease	none	Wurzbacher et al.[36]
Amine-functionalized proprietary resin	increase	na	decrease	na	Elfving et al.[19]
Amine-functionalized proprietary resin	increase	na	decrease	na	Elfving et al.[20]
Amine-functionalized CA silica fiber sorbents	increase	na	decrease	na	Sujan et al.[26]
Aminopolymer-impregnated hierarchical silica structures	increase	na	increase	na	Kwon et al.[23]
Amine-Impregnated MIL	increase	na	decrease	na	Rim et al.[28]

release it upon low temperature heat provision (100−200 °C). In this case, the active material is immobilized on a surface in an engineered contactor, which typically resembles a device for air treatment (e.g., air conditioning).[11] Both processes have their respective advantages and drawbacks and have so far been applied by a few companies in about a dozen pilot plants only (e.g., Carbon Engineering, Climeworks, Global Thermostat, Antecy, Hydrocell, Infinitree, Skytree).[11] Sabatino et al.[10] conclude that scrubbing of air with an aqueous alkali solution is inexpensive for the capturing section but suffers from a complex or energy-intensive regeneration step. In contrast, solid sorbent processes have the advantage of low-temperature sorbent regeneration. The setup of the process is modular and thus flexible in terms of operation and sizing but requires advanced sorbents, which are not produced at industrial scale and whose exact costs are unknown (estimated in the range $15−150/ton[12,13]). In this work, we focus on the solid sorbent DAC process, which is attracting most of the scientific and industrial interest.[14]

The growing academic body of literature on solid sorbent DAC has so far mainly focused on four main pillars: (1) the role of DAC technologies in the mitigation of climate change;[3,4,7,15−17] (2) the development of new materials capable of capturing CO_2 from air;[18−28] (3) the life-cycle assessment of DAC;[29,30] and (4) the economics of DAC technologies.[11,13,16,31,32] Note that the reference list above is not meant to provide a comprehensive overview of the rapidly expanding works on DAC but is rather exemplary. For that purpose, readers could refer to recent review papers.[24,33,34] So far little attention has been paid to investigate the DAC performance under varying ambient conditions (e.g., different geographic locations, varying seasons, daily fluctuations), despite these factors playing a pivotal role in the performance of the technology.[14] Recently, Terlouw et al.[30] has shown that the choice of location of a DAC system is a key factor for its global greenhouse gas removal potential, especially because of renewable heat and electricity availability. Moreover, there is an underlying thermodynamic behavior that controls the solid sorbent DAC performance at varying ambient conditions, notably temperature and humidity of the incoming air. First of all, the ambient temperature strongly affects the CO_2 adsorption on the material, which is an exothermic process. Higher air temperature leads to higher specific energy demand and lower productivity, especially at fixed regeneration temperatures; this is a direct consequence of the reduced cyclic capacity at higher air temperature. Second, the air humidity affects the performance of most solid sorbents currently considered for DAC (e.g., amine-functionalized sorbents, ion exchange resins), though in a more complex way: the coadsorption of water at high humidity levels leads to (1) increased adsorption capacities and improved reaction kinetics, resulting in larger capturing capacities per cycle; and (2) higher energy requirements during the regeneration since besides CO_2 also water must be desorbed.

Most academic work investigating the influence of temperature and humidity has been conducted in the realm of material science including both theoretical and small-scale experimental analysis under lab-conditions. Table 1 provides an overview of studies that took into account the impact of humidity or temperature on the sorbent. It highlights the counteracting effect of increased humidity on the energy and adsorption capacity, and the straightforward effect of the temperature on the CO_2 adsorption capacities. The studies suggest that materials used for solid sorbent DAC typically perform best in humid and cold conditions. However, for a carbon neutral DAC process, renewable energy supply is needed. These renewable resources are typically located at warm and dry locations (especially cheap solar resources). It follows that the availability of renewable energy and the ambient air conditions lead to a trade-off between an optimal DAC performance and an economical energy supply.

With this work, we aim at better understanding the effect of climatic conditions (i.e., geographic locations) on the optimal operation and design of solid sorbent DAC processes as well as on the associated energy supply system. We therefore complement and extend the studies on sorbents behavior and characterization at different ambient conditions with a process and system level perspective so far missing in the open scientific literature. We do this by bridging a robust, yet complex thermodynamic model of the process to a computationally efficient linear model, which can be used for hourly resolved system design and operation.

The remaining part of the paper is structured as follows. In section 2, we describe the mixed-integer linear model framework used to analyze the solid sorbent DAC process at different boundary conditions (space and time). In section 3, we first analyze the optimal operation and design of a standalone DAC unit, and, second, integrate the DAC unit in a multi-energy system with heat and electricity provided by renewable resources. Finally, section 4 presents the conclusions of this work.

2. MODELING FRAMEWORK FOR SOLID SORBENT DAC PROCESSES AT VARYING AMBIENT CONDITIONS

Ambient conditions vary significantly following daily and seasonal cycles; understanding DAC behavior under such

https://doi.org/10.1021/acs.iecr.2c00681
Ind. Eng. Chem. Res. 2022, 61, 12649−12667

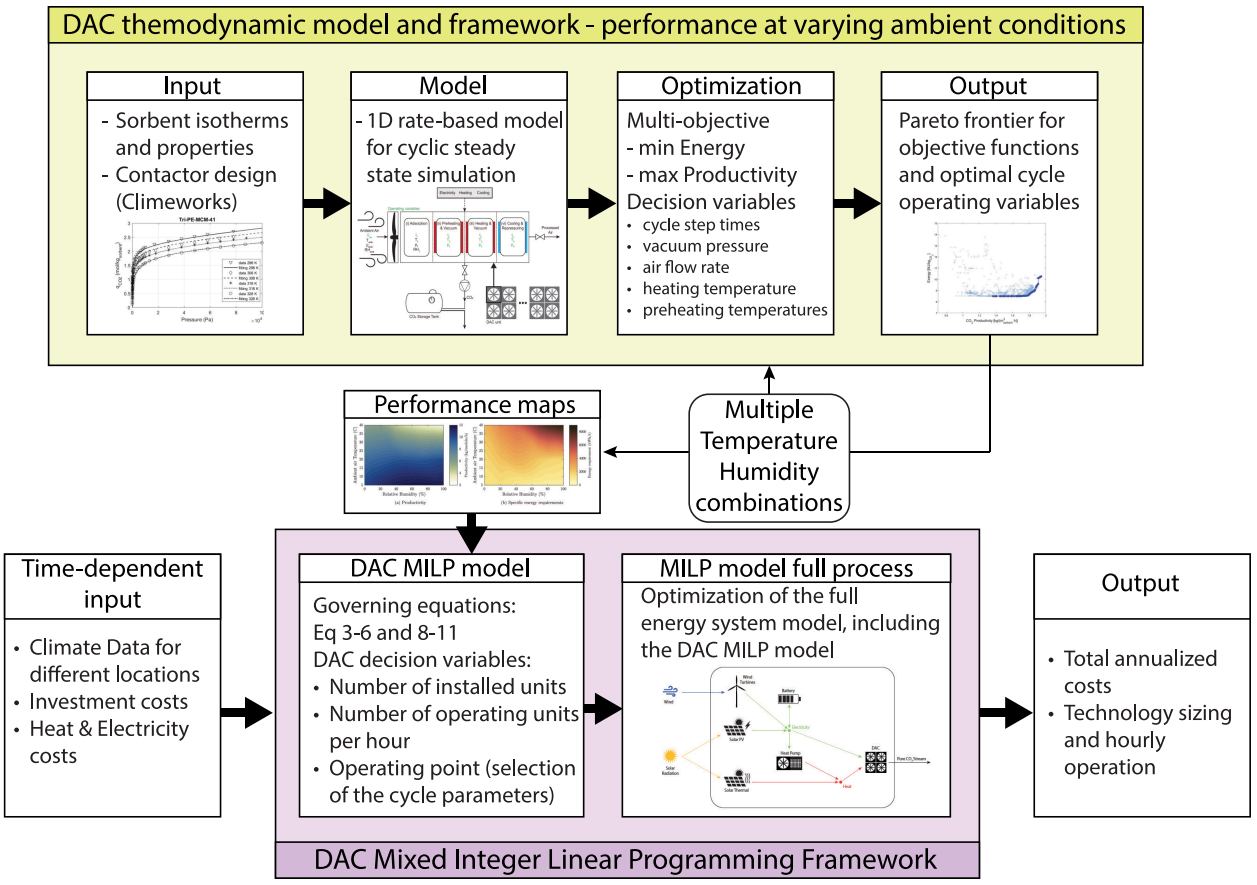

Figure 1. Modeling framework developed in this work to assess the performance of DAC at varying ambient conditions. The thermodynamic models adopted here and depicted in the top part of the figure were developed in the work of Sabatino et al.[10] The MILP modeling framework includes the DAC model and the overall system model.

conditions therefore requires a yearly time horizon with an hourly resolution. Clearly, the classical thermodynamic approach of simulating adsorption cycles with energy, mass and momentum balances discretized in space, and integrated in time is not viable in a similar framework: the computation of a full cycle and its CSS conditions requires significant computing time (typically in the order of minutes for CSS), which would make the analysis unfeasible when thousands (8760) of simulations must be performed. On the other hand, linear modeling, which is often used for complex time-discretized problems, has limited fidelity if not supported by thermodynamics; this can easily lead to wrong performance prediction. To tackle these shortcomings and properly evaluate the performance of a DAC process under varying ambient conditions, we developed a new modeling framework, which is shown in Figure 1. At the core of the method lies the interaction between a thermodynamic-based description of the process and its reformulation as a MILP. The thermodynamic framework (top box in Figure 1) is used to evaluate and optimize the performance of the DAC VTSA cycle for an assigned set of temperature−humidity combinations. It is important to note that the use of process optimization allows the user to identify the optimal working conditions, in terms of productivity and energy consumption, for any temperature−humidity combination. These results are then used to build model-based performance maps at different ambient conditions, which provide input to the hourly discretized MILP optimization problem (bottom box in Figure 1). Finally, the MILP model is run to identify the optimal design and operation of a stand-alone DAC process or of a full system where the process is coupled to the energy provision. This modeling framework preserves the physical behavior of the process while enabling the optimization of design and operation of DAC. In addition to productivity and energy consumption, the performance maps provide the set of associated optimal decision variables so that the optimal cycle configuration is known for every point. Accordingly, the modeling framework provides detailed insights on how the adsorption cycle needs to be operated.

It is worth noting that the thermodynamic modeling approach used here has been developed and applied to various processes in the past, for example, to DAC in Sabatino et al.,[10] to TSA in Joss et al.,[37] and to VPSA in Streb et al.[38] On the other hand, the key modeling contributions of this work are (i) the development of the MILP-DAC model, and (ii) the development of the overarching modeling framework shown in Figure 1. Accordingly, the remaining of this section describes the MILP-DAC model and its embedding in the overall framework (i.e., with respect to the possible DAC operating modes). The performance maps are described at the end of this section, while all details on the thermodynamic framework can be found in the references mentioned above (for clarity, the main balance equations are also reported in the Supporting Information).

Concerning the DAC cycle, we consider a VTSA process, which can be regarded as state-of-the-art for CO_2 capture from air with solid sorbents. This cycle consists of four different steps, that is, (i) adsorption of the CO_2 from ambient air, (ii)

https://doi.org/10.1021/acs.iecr.2c00681
Ind. Eng. Chem. Res. 2022, 61, 12649−12667

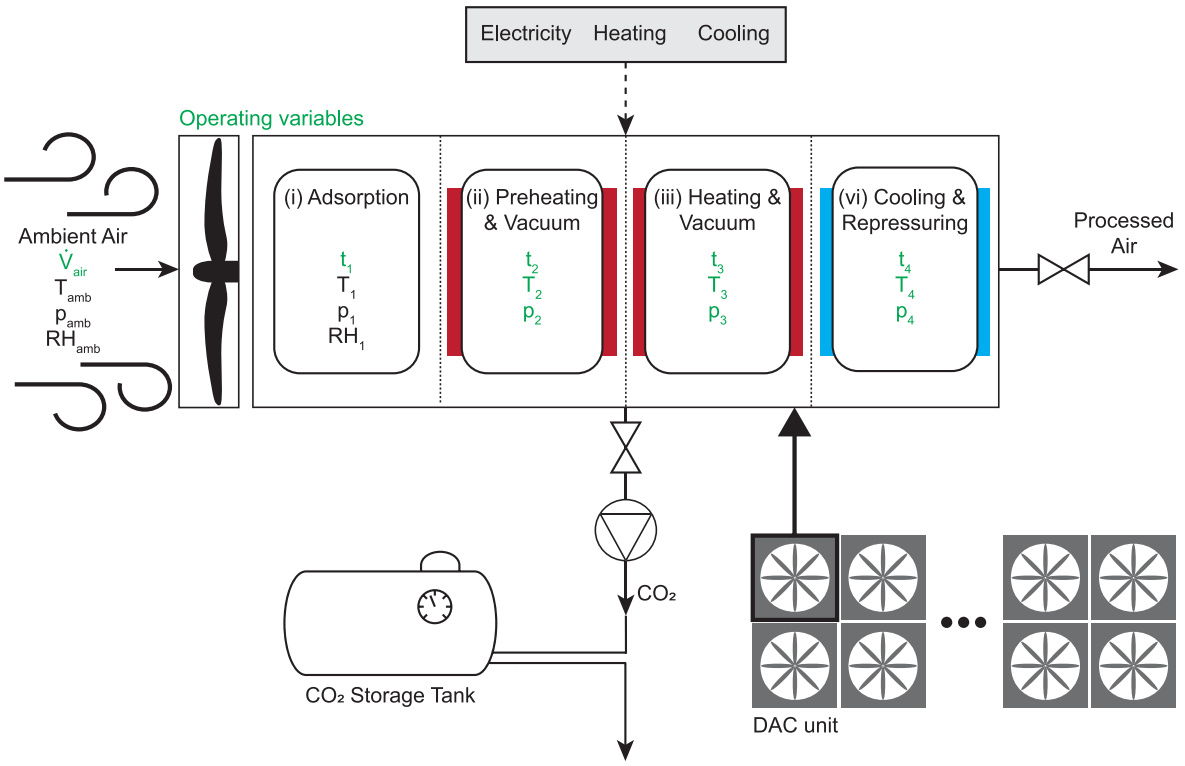

Figure 2. Scheme of a VTSA process for DAC including a representation of the four adsorption steps. Note that the process also produces water and other waste gases that were not illustrated for simplicity.

preheating while pulling a vacuum to remove most of the nitrogen, (iii) heating at vacuum conditions to produce a highly concentrated stream of CO_2, and (iv) repressurization and cooling (see Figure 2). Such a VTSA process is affected by both exogenous and controllable variables. The ambient air conditions are exogenous and vary over time and space. The controllable variables include design and operation choices such as the sorbent type, the contactor design, cycle times, pressure levels, and the regeneration temperature. Accordingly, a VTSA process will need to be equipped with a control strategy so as to guarantee high performance at varying exogenous variables by changing the operating parameters.

As discussed above, in the modeling framework we propose it is key to connect the VTSA performance to both ambient factors and process variables. For the formulation of the MILP-DAC model (bottom box in 1), the productivity−energy consumption relation obtained from the performance maps of the thermodynamic model is converted into an input−output relation between total required energy and captured CO_2 (eq 1). Therefore, the CO_2 output during the considered time-step (i.e., 1 h) O_t is function of the exogenous ambient conditions Θ_t, the total energy consumption E_t^{DAC}, and the number of working modules N_t. f is then translated into a mixed integer linear function as in eq 2, where performance parameters α_i and β_i depend on the ambient conditions and are obtained from the performance maps, and $s_{i,t}$ is a binary variable selecting a piece on the piece-wise defined function:

$$O_t = f(\Theta_t, E_t^{DAC}, N_t) \tag{1}$$

$$O_t = \sum_{i=1}^{I} s_{i,t}(\alpha_i(\Theta_t)E_t^{DAC} + \beta_i(\Theta_t)N_t) \tag{2}$$

Eq 2 needs further elaboration before implementation in an MILP model. The bilinearities in eq 2 are reformulated with the help of auxiliary variables $\tilde{E}_{i,t}^{DAC} = s_{i,t}E_{i,t}^{DAC}$ and $\tilde{N}_{i,t}=s_{i,t}N_t$ and can be written as in eq 3. The required auxiliary constraints are given in the Appendix. We therefore obtain

$$O_t = \sum_{i=1}^{I} \left(\alpha_i(\Theta_t)\tilde{E}_{i,t}^{DAC} + \beta_i(\Theta_t)\tilde{E}_{i,t}^{DAC}\right) \tag{3}$$

To ensure proper behavior of the model, additional constraints are needed:

- Selection of only one piece:

$$\sum_{i=1}^{I} s_{i,t} = 1 \tag{4}$$

- Boundaries for the energy input on each piece:

$$b_{i-1,t}s_{i,t}N_t \le \tilde{E}_{i,t}^{DAC} \le b_{i,t}s_{i,t}N_t \;\forall\; i \tag{5}$$

- Number of working modules at each time instance equal or smaller than total installed modules:

$$0 \le N_t \le N_{tot} \tag{6}$$

Moreover, the total energy demand E_t^{DAC} is decomposed into electric and thermal energy in line with the thermodynamic model:

$$E_{el,t}^{DAC} = \sum_{k=1}^{K} z_{k,t}(\gamma_k(\Theta_t)E_t^{DAC} + \delta_k(\Theta_t)N_t) \tag{7}$$

With $\hat{E}_{k,t}^{DAC} = z_{k,t}E_t^{DAC}$, we can follow the same linearization technique as above resulting in

https://doi.org/10.1021/acs.iecr.2c00681
Ind. Eng. Chem. Res. 2022, 61, 12649−12667

$$E_{\mathrm{el},t}^{\mathrm{DAC}} = \sum_{k=1}^{K} (\gamma_k(\Theta_t)\hat{E}_{k,t}^{\mathrm{DAC}} + \delta_k(\Theta_t) z_{k,t} N_t) \tag{8}$$

$$\sum_{k=1}^{K} z_{k,t} = 1 \tag{9}$$

$$a_{k-1,t} z_{k,t} N_t \le \hat{E}_{k,t}^{\mathrm{DAC}} \le a_{k,t} z_{k,t} N_t \tag{10}$$

It follows that the thermal energy demand can be calculated as

$$E_{\mathrm{th},t}^{\mathrm{DAC}} = E_t^{\mathrm{DAC}} - E_{\mathrm{el},t}^{\mathrm{DAC}} \tag{11}$$

Additional auxiliary variables are introduced to tackle the respective remaining bilinearities in eqs 5, 8, and 10, as reported in full model formulation provided in the Appendix.

Overall, eqs 3−6 and 8−11 define a generic MILP model of a VTSA DAC process with temperature- and humidity-dependent performance and variable operation points. To make the model compatible with all possible energy supply routes, the thermal energy can also be provided by ohmic heating. Therefore, the following equations hold:

$$E_{\mathrm{el},t} = E_{\mathrm{el},t}^{\mathrm{DAC}} + E_{\mathrm{th},t}^{\mathrm{DAC}} / \eta_{\mathrm{el,th}} \tag{12}$$

$$E_{\mathrm{th},t}^{\mathrm{DAC}},\ E_{\mathrm{el},t} \ge 0 \tag{13}$$

Figure 3 illustrates the resulting feasible operating space of a DAC process consisting of one, two, or three individual modules

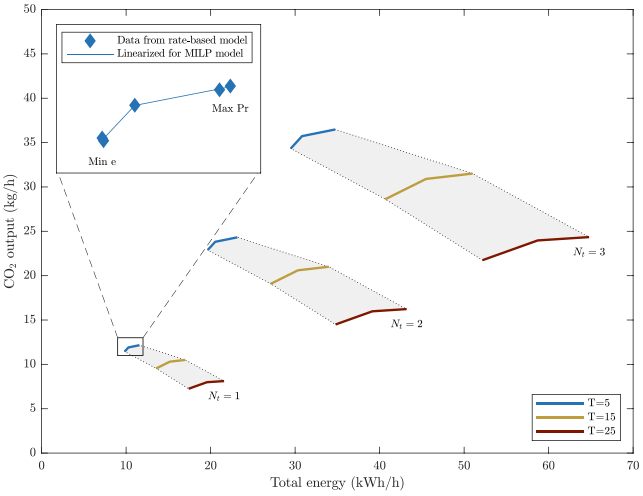

Figure 3. Operational space of a DAC unit consisting of three modules at 75% relative humidity and different temperatures. For each temperature−humidity combination, the feasible operating points are depicted by the colored lines. The gray areas contain the operational space for other temperatures. The small plot in the upper left corner shows the relationship between the thermodynamic rate-based model from Sabatino et al.[10] and the linearized data for the MILP model.

at three different temperatures, and the same humidity level (kept constant for clarity in the illustration). It is possible to move along the operation lines (i) by changing the operating parameters of the DAC unit, that is, moving from minimum energy to maximum productivity adjusting cycle times, vacuum pressure levels, and regeneration temperatures (each operational point corresponds to a set of operating parameters determined in the thermodynamic model); and (ii) by changing the number of working modules N_t. Eventually, the CO_2 output of one module is defined by the conditions of the ambient air, and the chosen energy input, which corresponds to a specific DAC operating point. The zoom-in in Figure 3 shows the comparison of the MILP-DAC performance (lines) with the data from the thermodynamic model (diamonds); there is very good agreement between the two.

It is worth noting that the model presented can be used for any sorbent for which performance data are available and performance maps are obtained. It thus offers a possibility to simulate a sorbent working at different locations or compare different sorbents for a specific location. Moreover, the model can be used under different ambient condition scenarios. When the ambient conditions are constant throughout the time horizon, the model will identify the optimal size (N_{tot}) and operating point, which will also be constant in time. When the ambient conditions vary throughout the time horizon, the model will identify the design size N_{tot}, and for every time instance, the number of working modules N_t, and the operating point, which will now vary in time.

The MILP model can be further manipulated to match the desired process control and the production process requirements. We consider here three possible operating configurations.

Operation Configuration 1 (OC1): Flexible CO_2 Production and Tunable Operating Parameters. This is the most flexible configuration to control the DAC process. First, the production of CO_2 can be flexible in time, that is, the total production over time horizon T must equal the CO_2 demand in the same period $\sum_{t=1}^{T} D_t$:

$$\sum_{t=1}^{T} O_t = \sum_{t=1}^{T} D_t \tag{14}$$

Second, the operating parameters can be adjusted to maintain the optimal operation for any given ambient condition. This case represents an optimally controllable DAC unit and mimics the ideal control system. It is worth stressing that, in this work, we do not aim to understand how this control system can be effectively achieved but to understand the DAC performance under such behavior. However, we do ensure that the operation is physically possible within the modeling framework by removing cycle times that are larger than the length of one time-step.

Operation Configuration 2 (OC2): Flexible CO_2 Production and Constant Operating Parameters. In this case, the CO_2 production can vary hourly, but the operating parameters are fixed during the whole time-horizon. The individual modules can be switched on and off, but their operation cannot be adapted to changing ambient conditions and thus run suboptimal. To model this behavior, eqs 3, 5, 8, and 10 need to be rewritten. The full formulation of OC2 can be found in the Supporting Information (Section 1).

Operation Configuration 3 (OC3): Constant CO_2 Production and Flexible Operating Parameters. In this configuration, the unit needs to maintain a constant CO_2 production level. The operating parameters however can vary. Eq 14 is thus rewritten as

$$O_t = D_t \tag{15}$$

In the Results section, we explore the different operation configurations for different ambient conditions, different locations, and for stand-alone vs system-integrated DAC processes.

https://doi.org/10.1021/acs.iecr.2c00681
Ind. Eng. Chem. Res. 2022, 61, 12649−12667

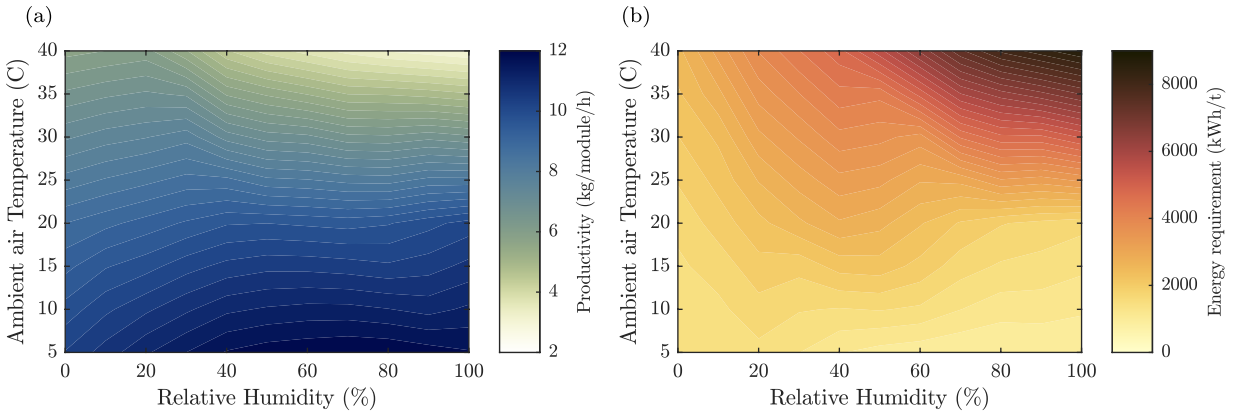

Figure 4. Productivity and specific energy requirements for maximal productivity optimization.

The mixed integer linear model presented requires data on the performance of a VTSA as a function of the exogenous variables and the respective control parameters. To this end, we simulated the process with a 1-D model, where the productivity and energy consumption are calculated starting from the cycle and sorbent characteristics. The 1-D model is rate-based and has been used and validated experimentally for multiple adsorption cycles. More details can be found in Sabatino et al., Cases et al., and Joss et al.[10,39−41] For the sorbent, we follow the approach of Sabatino et al.,[10] and consider an exemplary material, which was obtained by combining experimental data of four representative sorbents for direct air capture. This allowed us to study the average behavior of solid sorbents without focusing on a specific material (details on the exemplary sorbent calculations can be found in Sabatino et al. referring to case 2: E-A[10]). The isotherm parameters as well as the model parameters for the simulation are listed in Tables S1 and S2 in the Supporting Information. To obtain the data needed to fit $\alpha_i(\Theta_t)$, $\beta_i(\Theta_t)$, $\gamma_k(\Theta_t)$, and $\delta_k(\Theta_t)$, we carried out several multiobjective simulations of the VTSA DAC process, whose two competing objectives are productivity Pr and energy consumption e.[42] The problem is therefore defined as

$$\min_x(-Pr,\ e)$$
$$\text{subject to } \Phi \geq \Phi_{\text{spec}} \tag{16}$$

where x are decision variables (decision variables are adsorption, preheating and heating times, the vacuum pressure level, the air flow rate, and the heating and preheating temperatures), Φ the CO_2 (dry) purity, and Φ_{spec} the required minimum purity (here 95% vol). Details of the calculation of the productivity and the energy consumption, as well as the range of the decision variables, can be found in the Supporting Information (Section 1). To account for the influence of both temperature and humidity on the performance of the VTSA process, several cases were optimized by combining a range of ambient temperatures (5 °C, 20 °C, and 40 °C) with different humidity levels in the feed stream (0%, 22%, 43%, 75%, and 100%). It follows that multiple Pareto fronts were obtained for several fixed ambient conditions (the results are shown in Figure S2 in the Supporting Information).

Figure 4 shows the interpolation of the results in the investigated range of ambient conditions. As expected, the CO_2 capacity of the sorbent decreases with temperature, and therefore, the productivity is higher at low ambient temperature. In addition, the capacity increases with increasing humidity, especially for low temperatures. However, for temperatures above 30 °C, the productivity decreases with humidity. The reason is found in the trade-off between the two competing objectives of optimization. When having a higher humidity in the feed stream, more water has to be heated up during the regeneration; while for lower feed temperature, this is compensated by the sorbent capacity, for higher feed temperature, the capacity of the sorbent is low, and the heat required to heat up the water has a high effect on the overall energy consumption. Therefore, the process optimization keeps the energy requirement limited by allowing a loss in productivity.

3. RESULTS

In this section, we investigate the effect of ambient conditions at different locations on (i) a stand-alone DAC unit and (ii) a DAC unit embedded into an energy supply system relying on renewable resources.

3.1. Stand-Alone DAC. In this analysis, electricity and heat are provided from outside the system boundaries at constant prices. We identify the optimal DAC system design and operation by minimizing total system costs, which are the sum of investment and operational costs, for an arbitrary CO_2 demand of 10,000 tons/year. The operation variables of the DAC, that is, duration of the individual cycle steps, temperatures, and pressures, are selected through the choice of the operational point in the feasible operational space (see also Figure 3) further constrained by the chosen operational configuration. Therefore, we minimize the annualized total costs of the system (eq 17) subject to the CO_2 balance (eq 14 or 15) and the technology model (eqs 3−6 and 8−11):

$$\min C = \sum_{t=1}^{T}\left[p_{\text{el},t}E_{\text{el},t} + p_{\text{th},t}E_{\text{th},t}\right] + C_{\text{inv}} + C_{\text{main}} \tag{17}$$

s.t. eq 3−6, 8−11, and 14 or 15 where C denotes total annualized costs, $p_{\text{el,t}}$ and $p_{\text{th,t}}$ electric and thermal energy prices, respectively, and C_{inv} and C_{main} annualized investment and maintenance costs. Energy, investment, and maintenance costs as well as performance parameters at given ambient conditions are the only exogenous parameters of the model. The maintenance costs are assumed to be a constant fraction (4%) of the annualized investment costs for the DAC unit. Given the high uncertainties of the capital costs for DAC processes, we derive a fixed value for C_{inv} that results in total specific cost of 300 Euro/t CO_2 captured (this is calculated based on the average capturing costs for constant ambient conditions).

https://doi.org/10.1021/acs.iecr.2c00681
Ind. Eng. Chem. Res. 2022, 61, 12649−12667

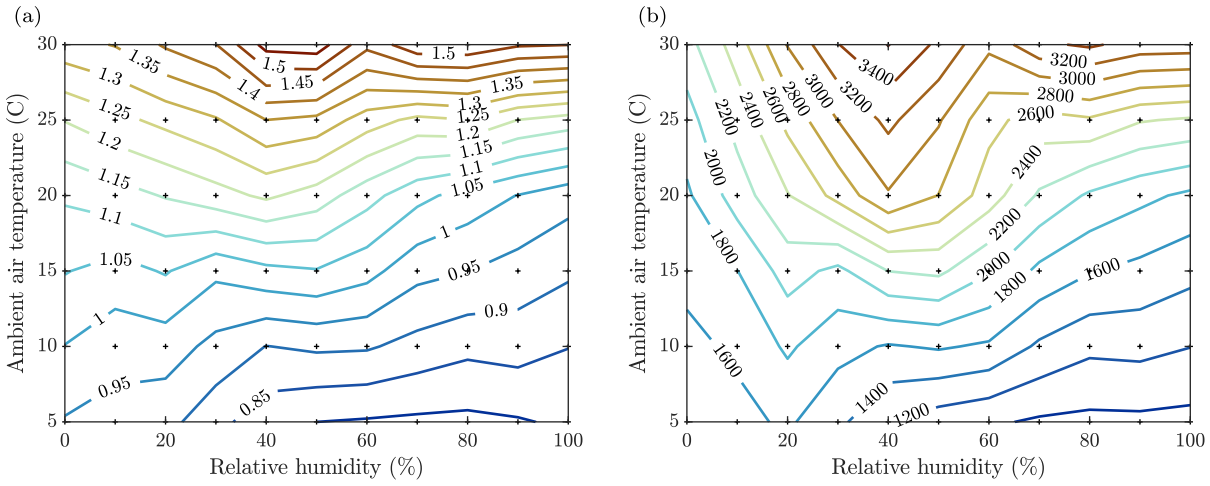

Figure 5. Normalized capturing costs and specific energy requirements at different ambient conditions.

Subsequently, we normalize all resulting total capture costs to this value and present relative results for all simulations. This way, the findings can be transferred to other capturing cost estimations. The underlying calculations for the investment costs and the assumptions about energy prices and maintenance costs can be found in Table S5 in the Supporting Information.

The cost minimization problem described is carried out for two overarching cases: First, we compute the performance of DAC for different fixed temperature−humidity combinations, that is, their values do not vary in time and are constant for every hour of the year. This allows us to understand the performance of DAC for different ambient conditions but independent from their change in time and space and of the DAC operation strategy. Second, for all operation strategies described in Section 2, we compute the performance of DAC for varying temperature and humidity over the year according to real weather data. To investigate the system at (i) temperate-humid, (ii) hot-humid, and (iii) highly variable ambient conditions, we used the weather data of The Netherlands (Schiphol), Spain (Barcelona), and California, US (Lancaster), respectively. Moreover, we evaluate the effects of pretreating air with water injection, similarly to what is done for gas turbines; this has the benefit of evaporative cooling and humidifying the inlet air stream. For all these analyses, we use a linear version of the more generic piece-wise linear model described before. As shown in the Supporting Information (Section 4), this simplification leads to very small deviations with respect to the full piece-wise model.

3.1.1. Performance of DAC for Different Time-Independent Ambient Conditions. Here, we solve the cost optimization of a DAC system for different, time-independent temperature−humidity combinations. In other terms, we keep $\Theta_t = \bar{\Theta}$ constant over a full year and let the model choose the optimal values for $\alpha_i(\bar{\Theta})$, $\beta_i(\bar{\Theta})$, $\gamma_k(\bar{\Theta})$, and $\delta_k(\bar{\Theta})$.

Figure 5 shows the normalized capturing costs and energy requirements for 66 cost optimizations with different temperature−humidity combinations. Each marker represents one optimization with the respective temperature and humidity level. The results are shown as contour lines for (a) specific normalized capturing costs and (b) specific total energy requirements.

The results suggest that the temperature is the major driver for both energy requirements and capturing costs. In fact, a 1 K increase in temperature leads to a 3.4% increase in specific energy requirements and a 2.0% increase in costs on average. These relationships are though nonlinear: the increase in specific energy requirement and cost is larger at higher temperature. The effect of higher temperatures on the capturing costs is caused by higher specific energy requirements and lower sorbent productivity. In contrast to temperature, humidity plays a subordinate role for the DAC performance. Both the specific total energy requirements and the capturing costs first increase with humidity, peaking between 40 and 60% and then decline again. The electric energy requirement follows the same shape but with steeper slopes while the thermal energy requirements increase in humidity only for dry conditions (below 30%) and reach a stable level for higher values (see Figure S3 in the Supporting Information). For the former, the reason lies in the higher CO_2 cyclic capacity with higher humidity: the presence of water reduces the partial pressure of CO_2 in the product thus requiring a lower vacuum level and therefore lower overall electricity consumption. However, there exists a trade-off between reducing the vacuum pressure to get a higher cyclic capacity and increasing the vacuum pressure to save energy. For moderate humidity (e.g., 40%), the electrical energy demand increases with higher temperature since the positive effects of the humidity during the adsorption and the higher CO_2 partial pressure during the desorption are limited. On the other hand, for lower temperatures, the vacuum pressure can be higher since the cyclic capacity is already high. As for the effect of humidity, the productivity increases with humidity up to 30−40% and remains thereafter approximately constant (see Figure S4b in the Supporting Information). The rising productivity and rising energy requirements with increasing humidity have two counteracting effects on the capturing costs: (i) because of a higher productivity, less units are required for a fixed CO_2 capturing amount resulting in lower overall investment costs; (ii) rising energy requirements increase the operating costs of the unit. Consequently, the share of investment costs in the total capturing costs is lowest for humidity levels of around 40% (see also Figure S4a in the Supporting Information) and accounts for 76% of total cost. The lowest overall capturing costs are reached for cold and humid conditions, where the temperature has a leading role; these results confirm previous studies on sorbent performance.[20,26,27]

3.1.2. Performance of DAC for Different Time-Independent Ambient Conditions with Pretreatment of Inlet Air. The results presented in the last section suggest that solid sorbent DAC performs better in humid and cold conditions. To improve

https://doi.org/10.1021/acs.iecr.2c00681
Ind. Eng. Chem. Res. 2022, 61, 12649−12667

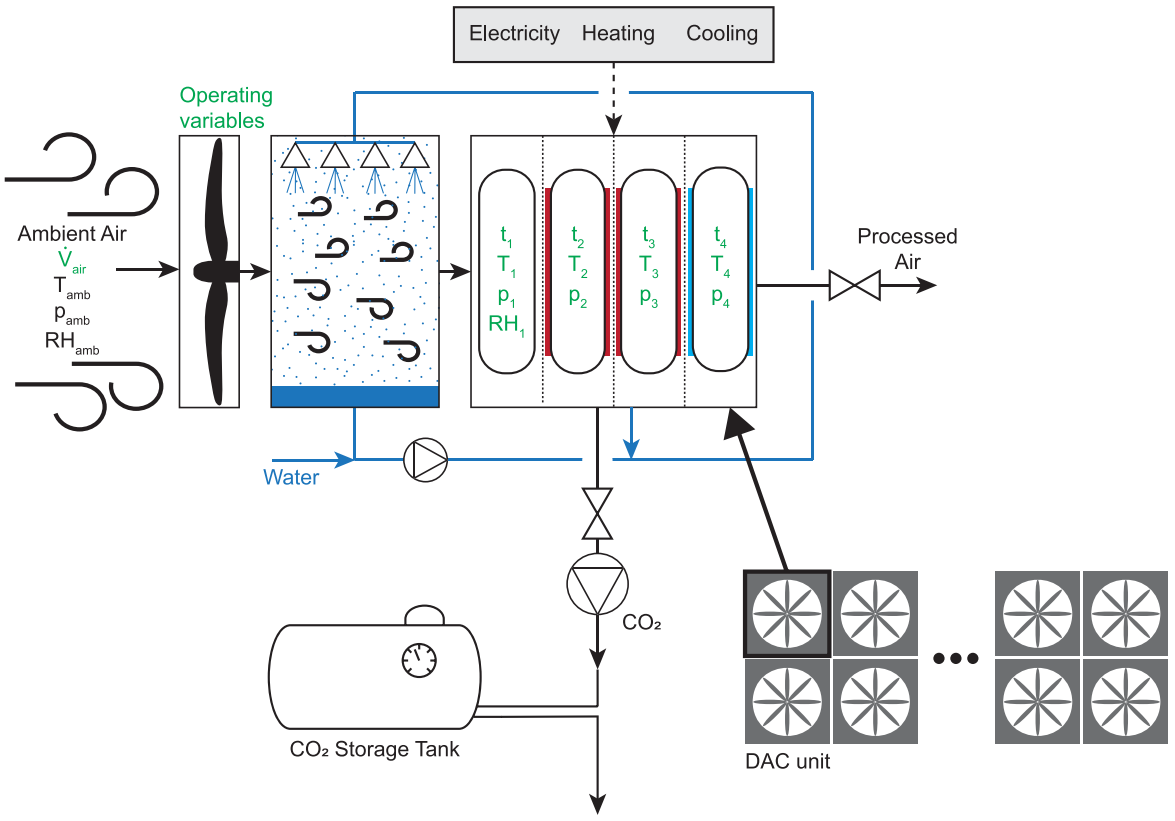

Figure 6. Scheme of a vacuum-temperature swing adsorption (VTSA) process for DAC including a representation of the four adsorption steps and a water treatment unit similar to the ones used in gas turbines.

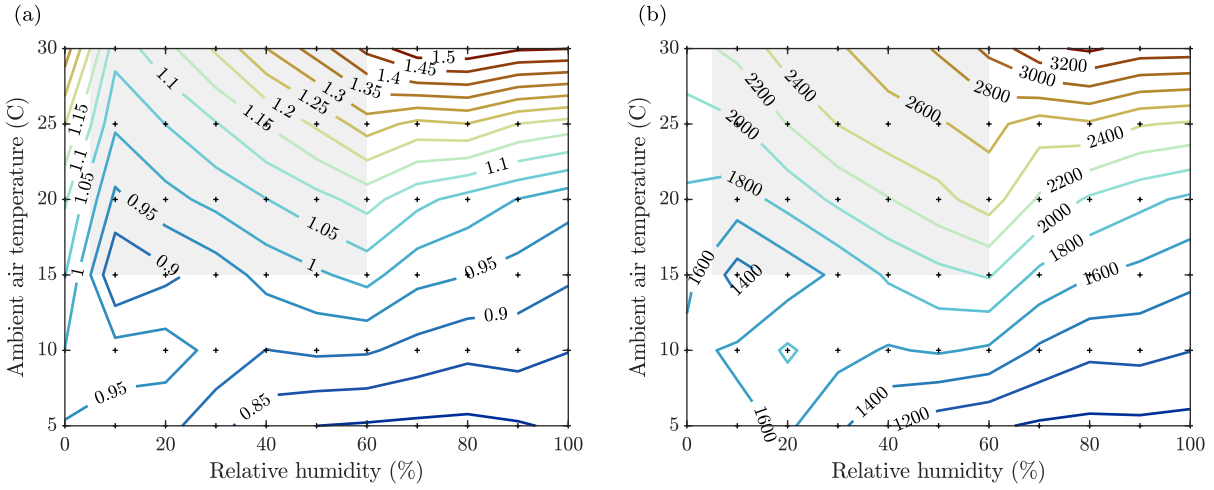

Figure 7. Capturing costs and energy requirements at different ambient air conditions allowing for spraying water in the inlet stream. The gray area indicates temperature−humidity-combinations for which spraying was possible. Note that humidity levels below 5% do not occur naturally and were thus left out.

the performance at these conditions, operational measures can be taken (see e.g. Drechsler and Agar[43]) or the humidity and temperature of the inlet air stream can be controlled. However, adding conventional cooling equipment would easily lead to detrimental pressure props, thus making impossible the treatment of large air flow rates. Here, and as shown in Figure 6, we propose an air-treatment unit as adopted in gas turbine inlet cooling: a simple water spraying process. This humidifies the incoming air while possibly cooling it without introducing significant pressure drops and costs. Moreover, the process is inherently designed for large flow rates. To this end, we have modified the DAC model presented earlier by adding the relative humidity of the air entering the DAC to the list of decision variables. Whenever the ambient temperature is above 15 °C, the humidity of the inlet air can be increased to 60% (this is an arbitrary value to emulate feasible humidification in short residence times). As a result, the temperature and humidity entering the adsorber bed become now controllable. Also in this case, we complement the mixed integer linear model with thermodynamics: the humidity and temperature changes are

https://doi.org/10.1021/acs.iecr.2c00681
Ind. Eng. Chem. Res. 2022, 61, 12649−12667

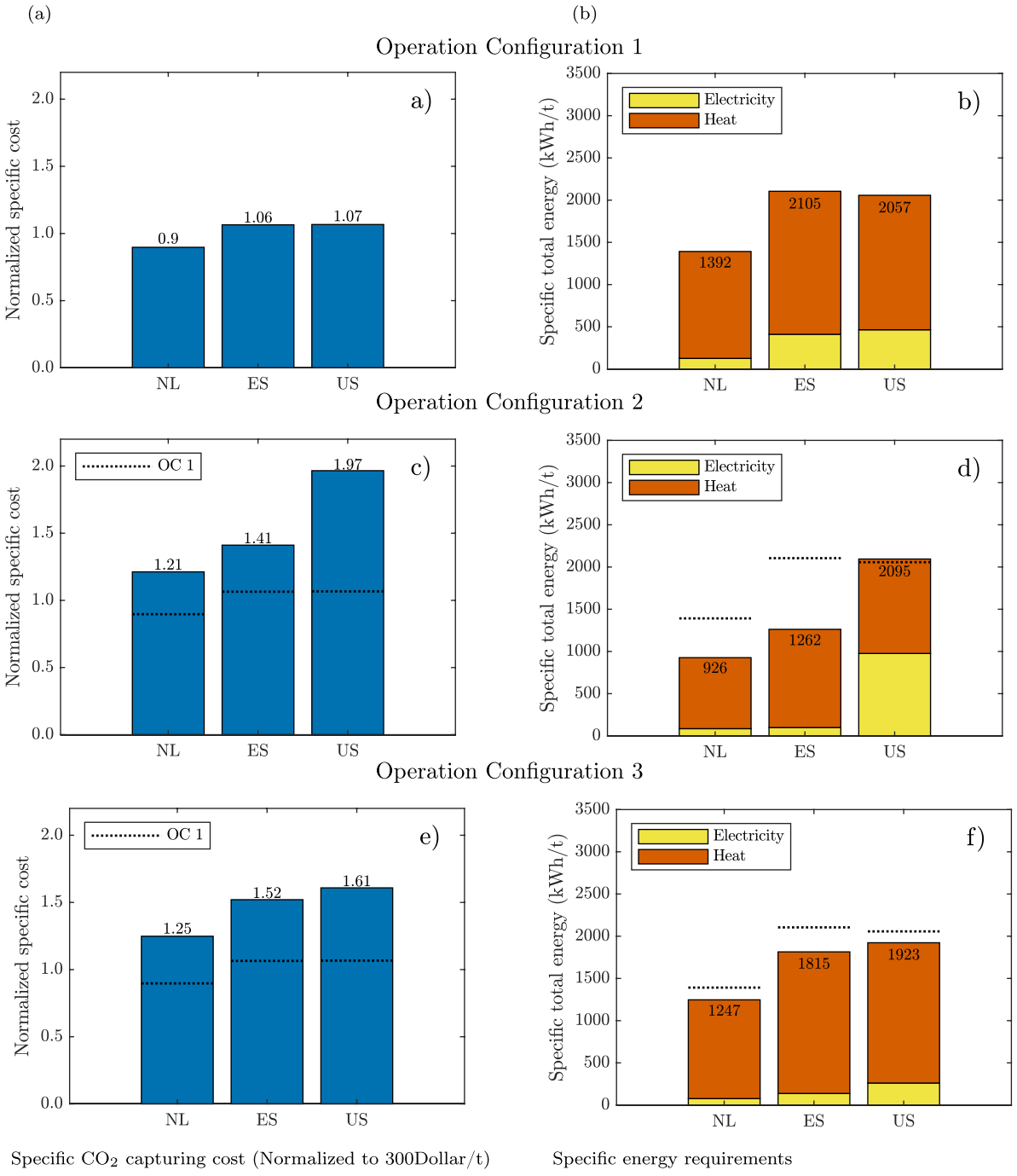

Figure 8. Cost and energy results for the stand-alone model for all operational configurations for (a, b) OC1, (c d) OC2, and (e, f) OC3.

computed using a linear interpolation of several combinations simulated in Aspen Plus. Given the simplicity of the process with respect to the DAC unit, the spraying of water is assumed to be costless with respect to both investment and operational costs. Similar to the analysis in the previous section, the operating variables are optimized for the respective fixed temperature−humidity combination and then fixed for every hour of the year. The full formulation of the model can be found in the Appendix.

The resulting performance isolines are shown in Figure 7. Generally, regions of low capturing costs and energy requirements expand, making the DAC process less sensitive to high ambient temperatures. For high temperature/low humidity levels, the benefits of water spraying are largest and yield a cost decrease of 21% (for 10% humidity/30 °C) and a total energy decrease of 29% (for 20% humidity/15 °C). These values mark an upper limit to the cost and energy improvements, which becomes particularly relevant for hot and dry locations.

For the water spraying, we estimate a water consumption of at most 1.5 t_{H2O}/t_{CO2}. This consumption can be critical, especially at dry and hot locations with scarce water resources. The effect of water usage on the surrounding ecosystem should not be underestimated and needs to be analyzed for every location individually based on its climatic and geographic features. However, it is also worth stressing that water can be effectively recovered in the regeneration steps, thus limiting the overall water consumption (net water production is also possible).

https://doi.org/10.1021/acs.iecr.2c00681
Ind. Eng. Chem. Res. 2022, 61, 12649−12667

3.1.3. Performance of DAC for Time-Varying Ambient Air Conditions. To study the effect of different climatic conditions on the DAC process with plausible humidity and temperature profiles, we selected three representative locations: Schiphol (The Netherlands), Barcelona (Spain), and Lancaster (US). Schiphol is characterized by a humid and temperate climate throughout the year with limited variability. Barcelona exhibits a similarly small variability of humidity and temperature; however, the average temperature is about 6 °C higher while humidity 20 percentage points lower. Lancaster has a similar average temperature as Barcelona, but its climate is significantly drier; more importantly, humidity and temperature exhibit high fluctuations even within single days. The input data as well as temperature and humidity profiles of all three locations are reported in Table S5 and Figures S8 and S9 in the Supporting Information. For simplicity, investment and maintenance costs are assumed to be equal at all locations. The findings are thus driven by different temperature and humidity profiles and the related differences in the process performance.

As in the section before, we minimize total annualized costs with an annual demand of 10,000 t of CO_2. All optimizations have the following configurations: (i) To reduce the run-time of the optimizations, full-year weather profiles are clustered into 100 typical days with a k-means algorithm. The days are clustered the same way for each model configuration of the same location. (ii) The minimum working temperature of the sorbent was assumed to be 5 °C, that is, the temperature has been fixed to 5 °C also for colder days. This is a conservative approach, as colder temperatures are beneficial for the CO_2 cyclic capacity. We decided to implement this approach to prevent infeasible operation close to the water triple point, especially for the adsorption step. There exist multiple strategies to operate DAC at low temperature, but these need to be devised specifically for a given design (one simple possibility is to keep the sorbent above 0 °C). (iii) The relationship between energy input and CO_2 capture is again modeled linearly with no breakpoints. For every location, we run the optimization for the three different operating configurations discussed before (OC1, OC2, OC3). Moreover, we investigate these three cases with and without water spraying. The results for OC1 to OC3 without water spraying are depicted in Figure 8. Table 2 contrasts the cases with water spraying with the cases without.

Table 2. Normalized Capturing Costs and Specific Energy Requirements in MWh/t of Different Model Configurations for a Stand-Alone DAC Operation

OC	water spraying	Schiphol (NL)	Barcelona (ES)	Lancaster (US)
		Normalized Capturing Costs		
OC1	no	0.90	1.07	1.07
	yes	0.90	1.05	0.99
OC2	no	1.22	1.42	1.97
	yes	1.21	1.34	1.59
OC3	no	1.25	1.52	1.61
	yes	1.19	1.38	1.28
		Specific Energy Requirements		
OC1	no	1.40	2.11	2.06
	yes	1.42	2.03	1.83
OC2	no	0.93	1.27	2.10
	yes	0.97	1.12	0.95
OC3	no	1.25	1.82	1.93
	yes	1.24	1.75	1.55

OC1: Flexible CO_2 Production and Tunable Operating Variables without Water Spraying. It can first be noted that Schiphol is the most suitable location for both the cost and energetic performance of the DAC: the capture costs at Schiphol are about 16% lower compared to Barcelona and Lancaster; likewise, the energy requirements are 33% lower. However, it can also be noted that the difference in costs among the various cases is limited and fully negligible between Lancaster and Barcelona. This is an inherent result of OC1, which allows for running the system at the operation points that are optimal for any temperature−humidity combination. In fact, at every location, the system works at full load over the whole modeled time-horizon, which is very much desirable for technologies with high investment cost share as for DAC. Hence, OC1 allows for exploiting the full potential of all installed units at all times, even though the ambient conditions at some time-steps result in unfavorable productivities and energy requirements. Figure S12 in the Supporting Information depicts the CO_2 output at all locations for different temperature and humidity levels, and it confirms that the ambient temperature is the main cost and energy driver for the operation of DAC systems. In contrast, humidity plays a subordinate role.

OC2: Flexible CO_2 Production and Non-tunable Operating Variables without Water Spraying. In practice, the flexible operation of OC1 requires advanced measuring equipment and control devices to set the operating variables optimally according to the ambient conditions; moreover, OC1 might not be viable when considering the dynamics of a specific DAC design. In contrast, in OC2 we optimize the set of operating variables once for the whole year and maintain these throughout. As long as the actual ambient conditions are around the values for which the variables are optimal, the DAC unit will work with a relatively high productivity and low energy requirements. When deviating significantly, the performance will worsen, respectively. This is however compensated by allowing for flexible production, that is, the technology is operated when most convenient. Figure 8 shows the results for cost and energy consumption. Moreover, Figures S14 and S15 in the Supporting Information show the correlation between CO_2 output and energy requirements for all three locations.

The cost performance of the DAC system worsens significantly at all three locations compared to OC1. Schiphol remains the site with lowest capturing costs and energy requirements. The increase in capturing costs and energy requirements in OC2 is largest in Lancaster; this is due to a higher variability in ambient conditions and thus demonstrates the limits of having one operating point for all temperature−humidity combinations. On the one hand, the operation of DAC becomes infeasible at temperatures or humidity levels far from the selected optimal operating point. On the other hand, the energy requirements increase more rapidly than in OC1 with flexible variables. As a consequence, the capture costs increase by 35%, 32%, and 84% for Schiphol, Barcelona, and Lancaster respectively, compared to OC1. The temperature remains the most important factor in explaining the productivity of an individual module and thus the overall capturing costs.

It can be noted that the specific energy requirements are lower compared to OC1 in Schiphol and Barcelona. First, it must be stressed that the objective function of the optimization is the total system cost, where energy appears as a price factor. Therefore, while in OC1 it is convenient to operate the DAC system at points where the energy consumption is not optimal (this reduces the total investment cost), in OC2 the system is

https://doi.org/10.1021/acs.iecr.2c00681
Ind. Eng. Chem. Res. 2022, 61, 12649−12667

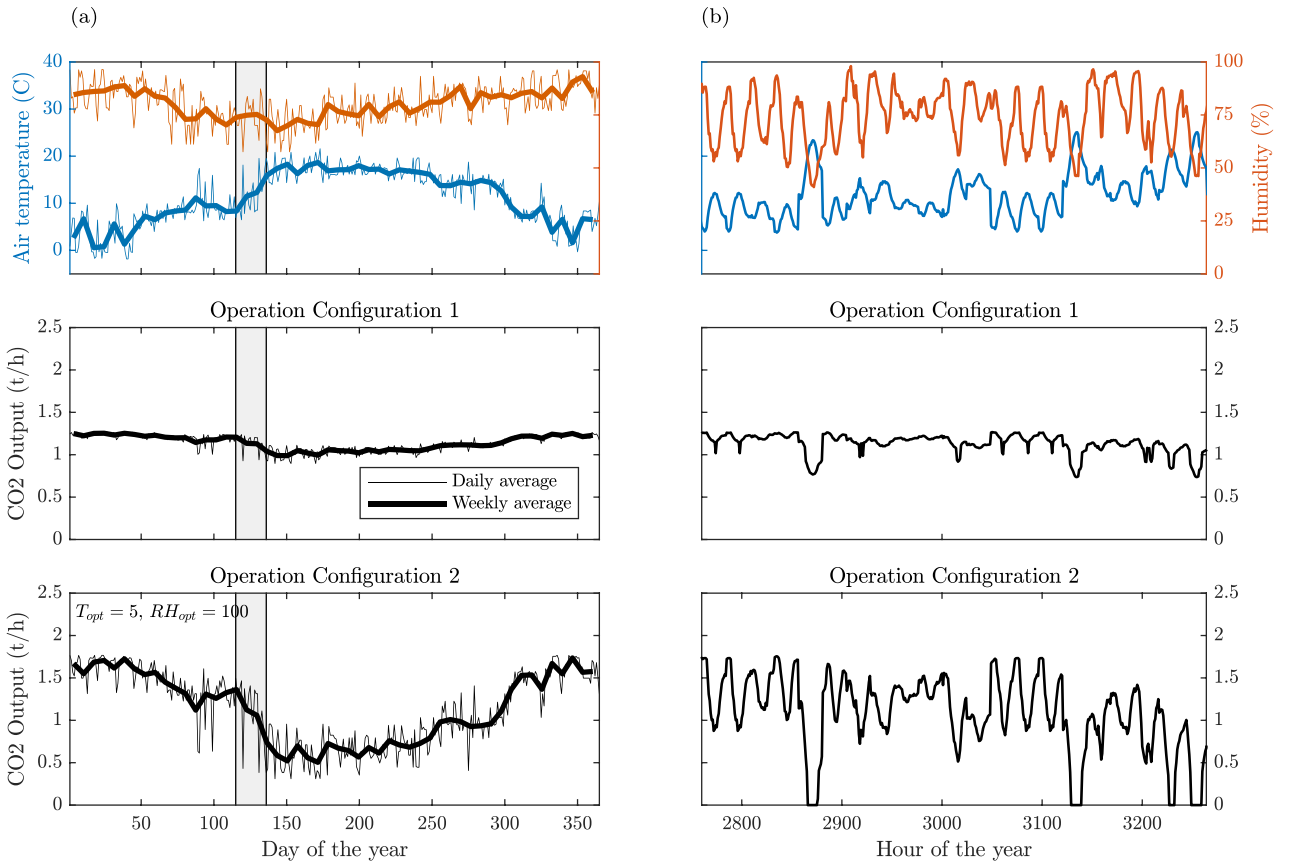

Figure 9. DAC operation in Schiphol (NL) (a) over the year and (b) in three sample weeks for OC1 and OC2. The gray area indicates the plotted time frame in panel b.

operated only for ambient conditions close to the optimal point. This mechanism, however, only works in Schiphol and Barcelona, but not in Lancaster, where both temperature and humidity fluctuate much more during the year and operation is even infeasible for the set of chosen operating variables.

Figure 9 provides additional insights on the underlying differences between OC1 and OC2 when the DAC system is installed in Schiphol (see Figures S17 and S18 in the Supporting Information for the other two locations); more specifically, it shows the operation of the DAC system in terms of CO_2 output over a year, and over three exemplary weeks. For OC1, the operation is overall stable, with a minor seasonal variation and a limited day/night cycle. This results from the capability of the DAC process to maintain optimal performance at varying ambient conditions. On the other hand, for OC2 the operation has a remarkable seasonal variation, low in summer and high in winter, as well as a remarkable day/night fluctuation. Notably, the DAC system is not producing any CO_2 during the warmest hours of the year. While on the one hand this results in a suboptimal use of the expensive equipment, on the other it offers a very simple solution to varying ambient conditions, which could possibly improve with the additional benefit of simple control algorithms. The difference between OC1 and OC2 is further amplified for Lancaster, that is, for locations with large variations in ambient conditions (see Figure S18): while OC1 allows for rather stable yearly and daily operation with minor adjustment for night−day cycles, OC2 features a high seasonal and daily change in CO_2 output.

OC3: Constant CO_2 Production and Tunable Operating Variables without Water Spraying. In this configuration, we require CO_2 to be steadily produced. Hence, production times cannot be shifted over the year, and favorable ambient combinations at different times cannot be exploited. However, operational variables can be tuned and kept to their optimal values. Results are shown in Figure 8e and f. Compared to OC1, costs increase significantly: 38%, 42%, and 49% in Schiphol, Barcelona, and Lancaster, respectively. The unit size in this configuration is now determined by the least efficient hour of the year, that is, the hottest and driest time-step. Once designed, the system can operate flexibly during all other hours of the year, for example, turning some units off to compensate for improved productivity or moving along the respective pareto lines. In fact, only during a small fraction of the whole year (<6%) are all units utilized. Clearly, this increases the costs significantly. Energy requirements decrease slightly because the capital cost is the driving force for the optimization: in OC2 and OC3, the optimization selects points on the pareto line with a lower specific energy requirement at the expense of a lower productivity.

By comparing OC3 and OC1, we can estimate the size and the maximal cost that a CO_2 storage tank could have while keeping its installation convenient. We find that the required size is in line with commercially available CO_2 storage tanks and that the maximum costs exceed significantly typical industry costs for small-scale CO_2 storage (see, e.g., Elementenergy mentioning specific storage cost between 600 and 2400 EUR/t_{CO2},[44] which is far from the acceptable maximal costs estimated in this work

https://doi.org/10.1021/acs.iecr.2c00681
Ind. Eng. Chem. Res. 2022, 61, 12649−12667

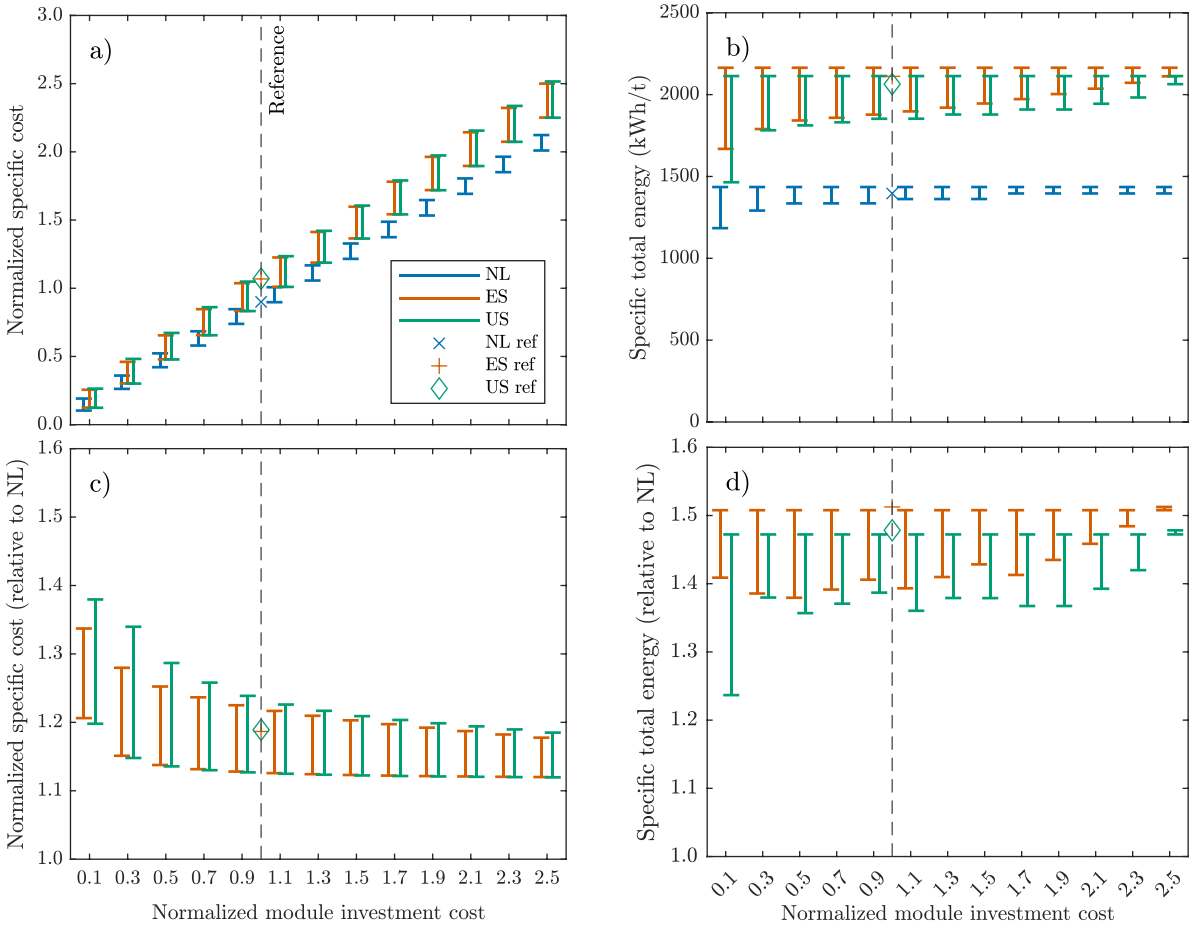

Figure 10. Capturing costs and specific energy demand for different price factors at three locations. The electricity price and the investment costs were varied between 0.1 and 2.5 of their initial value. The ranges indicated show the minimal and maximal energy requirements/costs for the respective minimal and maximal electricity costs. The upper graph depicts absolute values, the lower shows the ratio between Barcelona/Lancaster and The Netherlands.

(50000−90000 EUR/t_{CO2})) (see Supporting Information Section 8). Accordingly, a CO_2 storage tank appears to be a cost-effective and simple measure to cope with fluctuations in ambient conditions.

Benefit of Air Pretreatment (Water Spraying). High temperatures and fluctuations in the ambient air conditions drive up the DAC costs significantly due to suboptimal operation. This can be compensated by the pretreatment of the air inflow; the results for the three operation configurations presented before with and without water spraying are reported in Table 2.

At all locations, it is optimal to chose a maximal possible increase in humidity as this leads to the largest cooling effect. Figure S16 in the Supporting Information depicts the temperature−humidity conditions before and after spraying for model configuration 1. In humid conditions (Schiphol), the benefit of water spraying is limited for all operational configurations because the pretreatment is only utilized during a few hours. Accordingly, the cost and energy savings are minimal. On the other hand, in the case of Barcelona and Lancaster, and especially for OC2 and OC3, water spraying can significantly contribute to a better operation of the DAC, that is, whenever high fluctuation of temperature and humidity throughout the year are present. Overall, the water spraying reduces the range of temperature−humidity combinations, and thus, the process can operate more often closer to its optimum.

On average, the specific water consumption is 0.003, 0.02, and 0.15 t_{H2O}/t_{CO2}) in Schiphol, Barcelona, and Lancaster, respectively. The maximal economic cost per ton of water can be calculated by the differences in costs between the no water spraying and water spraying configurations. To be economically viable, these costs cannot exceed 311, 291, and 155 Euro per ton of water. This is much higher than typical water costs, which typically lie between 1 and 6 EUR/t_{CO2}.[45] The impact on the environment, however, should not be discarded, especially in regions with scarce water resources.

3.2. Sensitivity Analyses. We identified the following four main sources of uncertainty that could affect the findings of the previous analysis: (1) the performance of the solid sorbent at varying temperature and humidity, (2) the simplification of the DAC operation in a linear model and the respective modeling technique, (3) the investment and maintenance costs of the DAC unit, and (4) heat and electricity prices. Hereafter, we discuss the influence of these factors on our main findings.

3.2.1. Performance of Solid Sorbent Material. The productivity and energy requirements of the DAC process were obtained using the approach of Sabatino et al., where an exemplary sorbent was derived.[10] While the effect of temperature for different materials varies depending on the enthalpy of adsorption, the general trends hold for any adsorption material: capturing capacities decrease while energy requirements increase with increasing adsorption temperature (and fixed

https://doi.org/10.1021/acs.iecr.2c00681
Ind. Eng. Chem. Res. 2022, 61, 12649−12667

regeneration temperature). Thus, our results might change slightly with regards to the size of the effect, but not in their general trends. We tested two additional sorbent behaviors by (i) removing humidity dependencies from the data and (ii) inverting the humidity effect on the performance. These two cases aim at mimicking a sorbent, where CO_2 adsorption is not affected by H_2O adsorption, and a sorbent where CO_2 adsorption decreases with H_2O respectively. In both cases, the results remained substantially similar, confirming the leading role of temperature. Further information and the respective optimization results can be found in the Supporting Information (Figures S19 and S20).

3.2.2. From Thermodynamic to Linear Model. The linear model discards any nonlinear behavior in the operation at given ambient temperatures. However, it does take into account nonlinear relations between temperature−humidity states and the performance of the DAC. The model presented here simplifies the actual behavior of a DAC unit, but has no systematic bias at certain ambient conditions, that is, any different assumption will influence all simulations the same way. As for the 100-days clustering of weather data, we tested OC1 with original full-resolution profiles and the difference in capturing costs were smaller than 0.2%.

3.2.3. Investment Costs and Energy Prices. The objective function of the previous optimizations (eq 17), that is, the annualized total costs, is linear and homogeneous of degree 1 with regards to the investment costs and energy prices. Multiplying $p_{el,t}$, $p_{th,t}$, $C_{inv,an}$, and $C_{main,an}$ by the same factor would thus lead to an increase in the objective function by the same factor. Since the objective function is strictly monotonically increasing in these cost factors, the optimal value of the decision variables will not change for any price combination as long as their ratio is maintained. Consequently, the results obtained previously are equally true if all cost factors are multiplied by the same factor. However, if the ratio between electricity price, heat price, and investment costs changes, the optimal solution is also different. To study the effect of different ratios on our results, we simulated OC1 with varying cost ratios, that is, we fixed the electricity price and varied heat and investment costs between 0.1- and 2.5-times the initial assumption. The results are depicted in Figure 10, where for each investment cost and location, the energy requirements and capturing costs for the maximum and minimum heat price are shown. These are marked by the upper and lower ends of the whiskers. Additionally, the model outcomes from the previous section are plotted. As shown in Figure 10a and b, Schiphol remains the most suitable location for DAC over the whole range of cost combinations both in terms of energy consumption and capturing costs. Our previously obtained results are likely to hold for any price combination and future developments. Figure 10c and d give an indication of the relative difference between the three locations. It is important to note that the share of energy costs rise with smaller investment cost, and therefore, the model tends to pick operational points with lower energy requirements. However, even if investment costs of DAC were to decline drastically, the energy requirements in Barcelona and Lancaster are at least 1.2- and 1.4-times higher than in Schiphol (see lower plot in Figure 10). For larger investment costs, the share of energy costs in total capturing costs declines and thus also the model maximizes the productivity instead of minimizing energy, and the energy requirements approach their maximum for any tested heat price. This is indicated by smaller ranges in the upper plot of 10) for high module investment costs. The relative difference between the locations increases for smaller investment costs since Schiphol has the lowest energy requirements. Depending on the heat price, DAC is 1.21−1.34-times and 1.20−1.38-times as expensive in Barcelona and Lancaster, respectively. However, if investment costs are higher, this factor declines to 1.12 to 1.18 and 1.12 to 1.19 in Barcelona and Lancaster.

3.3. Direct Air Capture in a Multi Energy System. In the previous section, we studied the operation of a DAC unit in a stand-alone setup in which electricity and heat are provided from outside the model boundaries; however, it is essential that the energy supplied to the DAC is CO_2 neutral. Hence, we here investigate the DAC system when embedded in an autarkic multienergy system, where all heat and electricity is supplied by solar or wind resources. The system topology is shown in Figure 11. Electricity can be generated by onshore wind turbines or

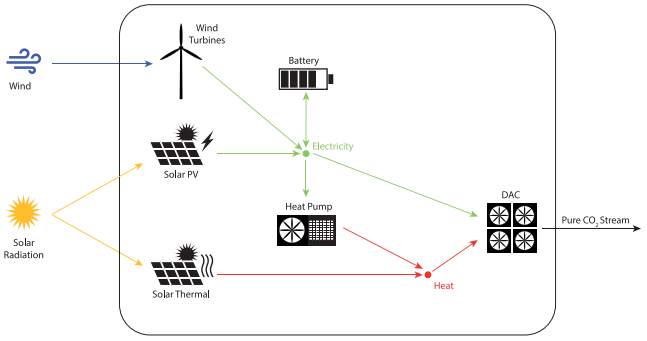

Figure 11. Energy system topology.

solar PV installations and stored in batteries if needed; heat is provided by either a heat pump or a solar-thermal installation. Additionally, electricity can be converted directly into heat by an ohmic heating within the DAC unit (see eqs 12 and 13). We take a greenfield approach and assume that all technologies need to be newly built, if selected by the optimization. The problem is formulated to minimize the total system cost J as a sum of investment cost J_c and operational costs J_o of all technologies:

$$\min J = J_c + J_o \tag{18}$$

The minimization problem is subject to the energy balance and technology dynamics and the full model formulation is found in the Supporting Information (Section 10) or in Gabrielli et al. and Weimann et al.,[46,47] and with this work we extend the technology portfolio by adding the MILP model of the DAC system presented earlier. Operational configuration 1 without water spraying was chosen for this analysis. Moreover, the technology costs are considered equal at all locations and thus the differences in outcome are again driven by different climatic conditions. All additional input data can be found in the Supporting Information (Section 10). Table 3 reports the cost optimal system design at the three considered locations. Additionally, Figure 12 shows the energy requirements of the DAC as well as the supply from the different generation technologies.

At all three locations, thermal energy is supplied by heat pumps or the built-in ohmic heating of the DAC unit. Solar thermal panels are never cost-optimal and thus not deployed. In Barcelona and Lancaster, the cost-optimal system design is very similar. Schiphol, however, is different because: (i) the DAC unit is composed of less modules due to the higher capturing productivity at lower temperatures; (ii) the total energy

https://doi.org/10.1021/acs.iecr.2c00681
Ind. Eng. Chem. Res. 2022, 61, 12649−12667

Table 3. Technology Sizes and Normalized Capturing Costs in the Optimal Energy System for All Three Locations

	Schiphol (NL)	Barcelona (ES)	Lancaster (US)
DAC (modules)	114	127	126
CO_2 Buffer Storage (t)	220.42	307.76	643.68
Photovoltaic (MWp)	1.40	4.22	3.84
Solar Thermal (MWp)	0.00	0.00	0.00
Wind Turbines (MW)	1.50	0.00	0.00
Battery (MWh)	4.05	7.95	7.99
Heat Pump (MWel)	0.37	0.45	0.44
Normalized Cost	1.12	1.32	1.29

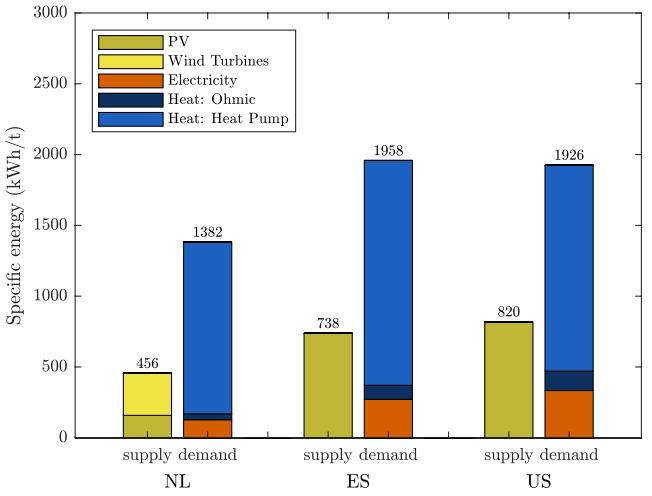

Figure 12. Energy generation (supply) and requirements of the DAC (demand) in the multi energy system.

requirements are lower compared to the other two locations; (iii) wind turbines are deployed for electricity generation in addition to solar PV as a consequence of the weather characteristics; and (iv) the battery is smaller thanks to the smoother electricity generation when coupling solar PV and wind turbines. The ohmic heating is deployed at all three locations during a few hours with high heat demand and sufficient electricity supply. This way, the size of the heat pumps can be reduced (see Figure 13).

The high availability of wind in The Netherlands balances the lower availability in solar irradiation and the capturing cost differences between Schiphol and the other two locations remain at about 16%, that is, similar to the stand-alone case. However, if wind energy becomes increasingly expensive or impossible to be deployed due to other reasons, the costs in The Netherlands increase above the other two locations (see also next section). This suggests, that cold and humid climates are beneficial only, if low-cost renewable energy is available. Additionally, the results show that the system in Lancaster has a higher need for flexibility, that is, a larger battery and a larger CO_2 storage. This allows for limiting the size of the DAC unit. More specifically, storage enables the optimal use of low temperature hours and prevent the operation in inefficient conditions. Adding costs for CO_2 storage capacity narrows the gap between Barcelona and Lancaster in terms of total capturing costs.

3.3.1. Sensitivity Analyses. The results presented in the previous section are indeed dependent on the cost assumptions of the respective generation and storage technologies. The total cost, that is, the objective function of the optimization, is linear and homogeneous of degree 1 in the technology investment costs as for the stand-alone case. Consequently, the absolute level of the costs are irrelevant, but the ratio between them determines the optimal solution. We have therefore investigated how changes in the investment costs of one individual technology and constant other costs affect the system design. Figure 14 and 15 show the results for all relevant generation and storage technologies. Figure 14a shows that wind turbines are deployed in The Netherlands for investment costs up to 3-fold the initial assumption, while they are not installed at the other two locations, even if solar PV costs increase 4-fold. If wind power is infeasible in The Netherlands, for example, due to area restrictions or prohibitively high prices, the better performance

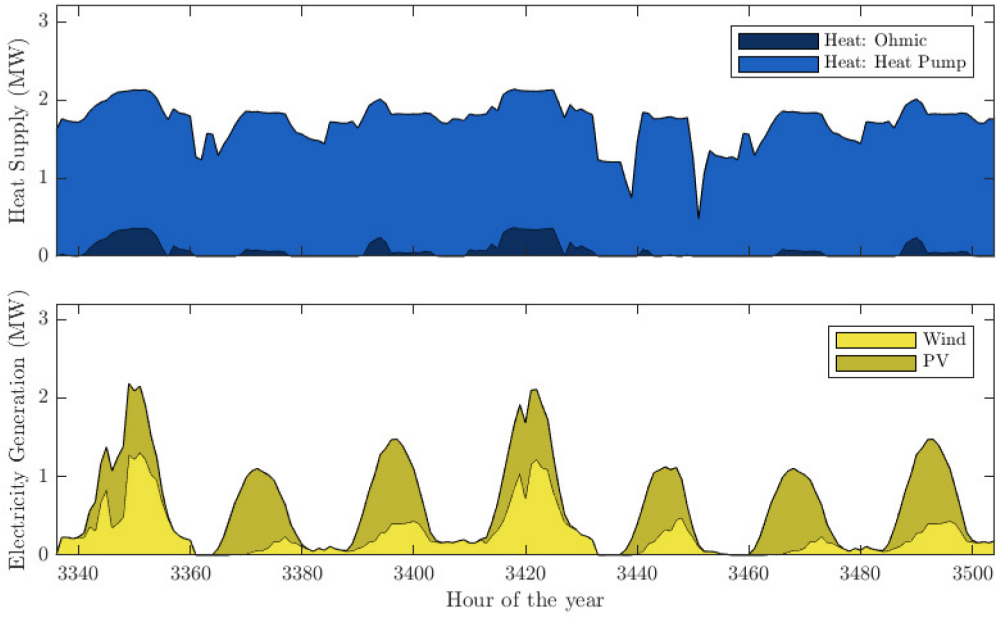

Figure 13. Electricity generation and heat supply over time for an exemplary week in April in The Netherlands.

https://doi.org/10.1021/acs.iecr.2c00681
Ind. Eng. Chem. Res. 2022, 61, 12649−12667

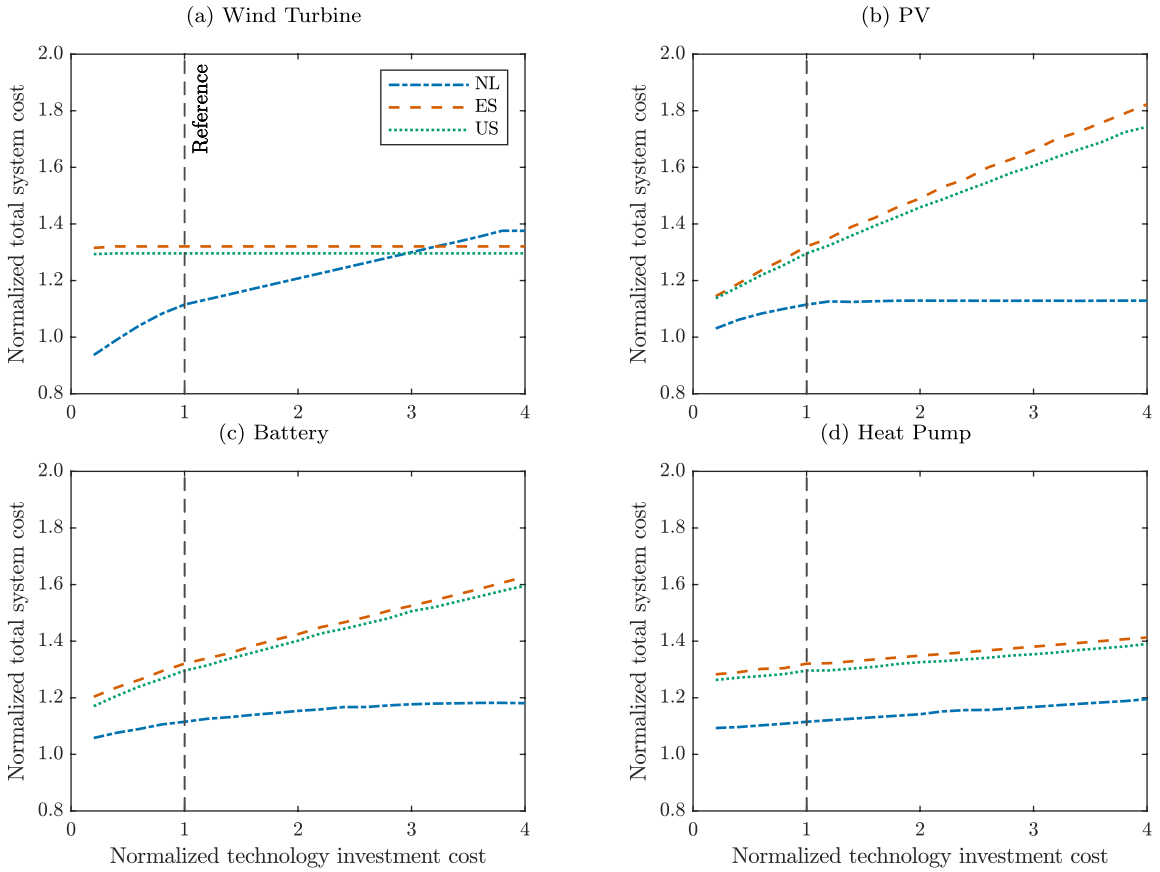

Figure 14. Total normalized system costs for different technology investment costs. The investment costs (reference) were varied between 0.1 and 2.5 of their initial value. Note that solar thermal was left out since it is never cost optimal to be built.

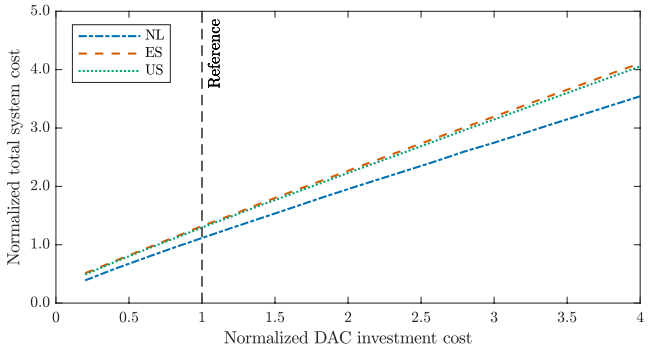

Figure 15. Total normalized system costs for different DAC investment costs. The investment costs (reference) were varied between 0.1 and 2.5 of their initial value.

of the DAC does not compensate for the higher expenses for electricity generation by solar PV. Since all heat supply to the DAC unit comes from electricity, either directly or through heat pumps, the PV investment costs play a major role at all locations. In fact, there is a linear relationship between investment costs into PV and capturing costs in Barcelona and Lancaster. In Schiphol on the other hand, higher PV costs lead to a scaling up of wind generation and thus the importance of PV decreases. This fact leads to larger differences between capturing costs for higher PV costs at locations with good wind resources. The effect of the battery investment costs exhibits a similar pattern: batteries need to be larger in single-technology systems, and in Schiphol, an increase of battery investment costs has a smaller effect on overall capturing costs than at the other two locations. The differences in capturing costs between The Netherlands and the other two locations thus increases for higher battery costs. Finally, for all three locations, the investment costs of the heat pump do not affect the total system costs significantly. The analysis has shown that the impact of energy supply costs on the overall capture cost is rather limited. Even for extreme cost decreases of the supply technologies, overall capture cost would only decrease slightly. Thus, the largest potential lies in cost decreases of DAC itself. This fact is also depicted in Figure 15 showing the sensitivity of the capturing costs dependent on the investment cost of the DAC unit. For DAC investment costs larger than the initially assumed value, Barcelona remains the most expensive location in terms of capturing costs, followed by Lancaster and Schiphol. Therefore, a change in DAC investment costs does not alter the conclusions drawn before.

4. CONCLUSIONS AND RECOMMENDATIONS

In this work, we have investigated the performance of an exemplary VTSA DAC process under varying ambient conditions, that is, temperature and humidity. More specifically, we have computed the energy consumption and the minimum system costs of the VTSA for multiple temperature−humidity combinations, and for three exemplary locations (The Netherlands, Spain, and California), where the ambient conditions are different both in terms of average values and daily/yearly profiles. Moreover, we have assessed three different approaches to operate the DAC system under varying ambient conditions, representing different control configurations and plant layouts. In addition, we have investigated the possibility of adopting

https://doi.org/10.1021/acs.iecr.2c00681
Ind. Eng. Chem. Res. 2022, 61, 12649−12667

evaporative cooling for the incoming air via simple water spraying. Finally, we have analyzed the system when accounting for the design and operation of the full CO_2 chain, that is, when the DAC process is coupled to a renewable-based energy supply system.

To enable this analysis, we have developed a new modeling framework that connects thermodynamic models to mixed-integer linear programming. More specifically: (i) we have synthesized a reliable, yet generic mixed integer linear model of a VTSA DAC process that, starting from optimized thermodynamic simulations, computes the process performance for varying ambient conditions; (ii) we have embedded the linear model into a design and operation MILP optimization of a stand-alone DAC system (i.e., electricity and heat are provided from outside the system boundaries); and (iii) we have integrated the DAC linear model in a large multienergy MILP model that is capable of optimizing the full energy supply system. These three methodological contributions will hopefully enable further studies on the operation of DAC technologies under different climatic conditions. We would like to stress that our work does not consider changes in adsorption kinetics at varying temperature and humidity, as a constant linear driving force was used in the simulations. This might be particularly important for cold regions, and it could be embedded in the model developing new performance maps at varying diffusion rates.

With this work, we show that when focusing on the stand-alone DAC process the annual average ambient temperature is the main climatic driver for both capturing costs and energy requirements. Surprisingly, humidity plays a subordinate role; this holds true for sorbents where CO_2 adsorption is enhanced by water as well for those that are negatively affected by water. In cold and humid climates, the capturing costs and energy requirements can be significantly lower than warmer locations: we found that the cost and the energy consumption of DAC deployed in The Netherlands are about 16% and 33% lower compared to Spain or California, respectively. This general trend remains true over a wide range of model setups and cost assumptions.

We found that the operation configuration significantly affects the performance of the DAC: a process where the operation variables can be optimally tuned to match varying ambient conditions shows the best performance but also requires an advanced control strategy that might not necessarily be viable when considering the system dynamics. Adding CO_2 storage to the system allows for an additional degree of flexibility, which could further enhance the performance or could limit the need of advanced control strategies. Notably, the optimal CO_2 storage is limited in size and costs.

We also found that air pretreatment with water spraying is always beneficial in terms of energy consumption and costs. However, water availability needs to be taken into account when designing such a DAC system.

When integrating the DAC process with the renewable-based energy supply (both electricity and heat), we can conclude that cold and humid locations are cost-efficient for DAC only if renewable energy can be supplied at low costs. In fact, we have shown that there is a significant trade-off between better DAC performance at cold locations and larger renewable resources at warmer locations. The worse performance of the DAC unit can be outweighed by high and inexpensive availability of renewable energy.

Accordingly, we can draw the following recommendations:

- DAC sorbents behavior at varying climatic conditions, especially at varying humidity, is still not fully understood and adequately investigated. However, the process performance is significantly affected by ambient conditions. Material scientists should consider this when synthesizing and characterizing sorbents.
- The optimal operation of VTSA DAC under time-varying ambient conditions requires adequate control algorithms and instruments. These have to be synthesized for specific process designs and associated dynamics. The vast research community of control systems should consider contributing to this research gap.
- The design of DAC technologies should take into account the fact that operation will inevitably take place under varying ambient conditions, varying electricity generation (i.e., electricity prices), and, likely, varying CO_2 demand.
- Whenever possible, DAC systems should be assessed along with the energy supply system, which can significantly affect the optimal design and operation of the process.

APPENDIX

Full Formulation of the Linear DAC Model

Bilinearities of the form aT, with a being a binary and T a continuous or integer variable with zero as its lower bound, can be substituted by an auxiliary variable and two additional constraints[48] to suit a MILP framework:

$$aT = \tilde{T} \tag{19}$$

$$0 \le \tilde{T} \le aT_{\max} \tag{20}$$

$$T - T_{\max}(1 - a) \le \tilde{T} \le T \tag{21}$$

We introduce the following auxiliary variables: $\tilde{N}_{\text{tot},\,i,\,t} = s_{i,t}N_{\text{tot}}$, $\hat{N}_{k,t} = z_{k,t}N_t$, and $\hat{N}_{\text{tot},k,t} = z_{k,t}N_{\text{tot}}$ and formulate the subsequent constraints:

$$0 \le \tilde{N}_{i,t} \le s_{i,t}N_{\text{tot}} \tag{22}$$

$$0 \le \hat{N}_{k,t} \le z_{k,t}N_{\text{tot}} \tag{23}$$

$$N_{\text{tot}}^{\min} \le \tilde{N}_{\text{tot},i,t} \le s_{i,t}N_{\text{tot}}^{\max} \tag{24}$$

$$N_{\text{tot}}^{\min} \le \hat{N}_{\text{tot},k,t} \le z_{k,t}N_{\text{tot}}^{\max} \tag{25}$$

$$N_t - N_{\text{tot}}(1 - s_{i,t}) \le \tilde{N}_{i,t} \le N_t \tag{26}$$

$$N_t - N_{\text{tot}}(1 - z_{k,t}) \le \hat{N}_{k,t} \le N_t \tag{27}$$

$$N_{\text{tot}} - N_{\text{tot}}^{\max}(1 - s_{i,t}) \le \tilde{N}_{\text{tot},i,t} \le s_{i,t}N_{\text{tot}}^{\max} \tag{28}$$

$$N_{\text{tot}} - N_{\text{tot}}^{\max}(1 - z_{k,t}) \le \hat{N}_{\text{tot},k,t} \le z_{k,t}N_{\text{tot}}^{\max} \tag{29}$$

The remaining equations are then:

$$O_t = \sum_{i=1}^{I} \left(\alpha_i(\Theta_t)\tilde{E}_{i,t}^{\text{DAC}} + \beta_i(\Theta_t)\tilde{N}_{i,t}\right) \tag{30}$$

$$\sum_{i=1}^{I} s_{i,t} = 1 \tag{31}$$

$$b_{i-1,t}\tilde{N}_{i,t} \le \tilde{E}_{i,t}^{\text{DAC}} \le b_{i,t}\tilde{N}_{i,t} \;\forall\; i \tag{32}$$

https://doi.org/10.1021/acs.iecr.2c00681
Ind. Eng. Chem. Res. 2022, 61, 12649−12667

$$E_{\mathrm{el},t}^{\mathrm{DAC}} = \sum_{k=1}^{K} \left(\gamma_k(\Theta_t) \hat{E}_{k,t}^{\mathrm{DAC}} + \delta_k(\Theta_t) \hat{N}_{k,t} \right) \tag{33}$$

$$\sum_{k=1}^{K} z_{k,t} = 1 \tag{34}$$

$$a_{k-1,t} \hat{N}_{k,t} \leq \hat{E}_{k,t}^{\mathrm{DAC}} \leq a_{k,t} \hat{N}_{k,t} \tag{35}$$

$$E_t^{\mathrm{DAC}} = \sum_{i=1}^{I} \tilde{E}_{i,t}^{\mathrm{DAC}} \tag{36}$$

$$E_{\mathrm{th},t}^{\mathrm{DAC}} = E_t^{\mathrm{DAC}} - E_{\mathrm{el},t}^{\mathrm{DAC}} \tag{37}$$

■ ASSOCIATED CONTENT

Supporting Information

The Supporting Information is available free of charge at https://pubs.acs.org/doi/10.1021/acs.iecr.2c00681.

Additional data and figures, details on the thermodynamic model, other specifications of the mixed integer model, formulation of the mixed-integer multi-energy system model (PDF)

Performance data of the sorbent (ZIP)

■ AUTHOR INFORMATION

Corresponding Author

Matteo Gazzani − *Utrecht University, 3584 CB Utrecht, The Netherlands;* orcid.org/0000-0002-1352-4562; Email: m.gazzani@uu.nl

Authors

Jan F. Wiegner − *Utrecht University, 3584 CB Utrecht, The Netherlands*

Alexa Grimm − *Utrecht University, 3584 CB Utrecht, The Netherlands*

Lukas Weimann − *Utrecht University, 3584 CB Utrecht, The Netherlands*

Complete contact information is available at: https://pubs.acs.org/10.1021/acs.iecr.2c00681

Notes

The authors declare no competing financial interest.

■ ABBREVIATIONS

CDR = carbon dioxide removal
CSS = cyclic steady state
DAC = direct air capture
MILP = mixed integer linear program
OC = operational configuration
PEI = polymeric amines and polyethylenimines
TSA = temperature swing adsorption
VTSA = vacuum-temperature swing adsorption
VPSA = vacuum-pressure swing adsorption

■ MATHEMATICAL SYMBOLS

$a_{k,t}$ = upper limit of piece in piece-wise affine input−input relation
$a_{k-1,t}$ = lower limit of piece in piece-wise affine input−input relation
$b_{i,t}$ = upper limit of piece in piece-wise affine input-output relation
$b_{i-1,t}$ = lower limit of piece in piece-wise affine input-output relation
C = annualized total costs of DAC
C_{inv} = annualized investment cost of DAC
C_{main} = annualized maintenance cost of DAC
$E_{\mathrm{el,\,t}}$ = total electric energy demand
$E_{\mathrm{el,\,t}}^{\mathrm{DAC}}$ = electric energy demand of DAC unit
$E_{\mathrm{th,\,t}}$ = thermal energy demand before ohmic heating
$E_{\mathrm{th,\,t}}^{\mathrm{DAC}}$ = thermal energy demand of DAC unit
$\hat{E}_t^{\mathrm{DAC}}$ = total energy demand of DAC unit
$\tilde{E}_{i,t}^{\mathrm{DAC}}$ = auxiliary variable for total energy demand of DAC unit
$E_{i,t}^{\mathrm{DAC}}$ = auxiliary variable for total energy demand of DAC unit
I = total number of pieces of piece-wise affine input−output relation
K = total number of pieces of piece-wise affine input−input relation
N_t = number of modules switched on
$\tilde{N}_{i,t}$ = auxiliary variable for number of modules switched on
$\hat{N}_{k,t}$ = auxiliary variable for number of modules switched on
N_{tot} = number of installed modules
$\tilde{N}_{\mathrm{tot,\,i,\,t}}$ = auxiliary variable for number of installed modules
$\hat{N}_{\mathrm{tot,i,t}}$ = auxiliary variable for number of installed modules
$N_{\mathrm{tot}}^{\mathrm{max}}$ = maximum of installed modules
$N_{\mathrm{tot}}^{\mathrm{min}}$ = minimum of installed modules
O_t CO_2 = output in time-slice t
$O_{\mathrm{dem,\,t}}$ CO_2 = demand in time-slice t
$p_{\mathrm{el,\,t}}$ = electricity price
$p_{\mathrm{th,\,t}}$ = heat price
$s_{i,t}$ = binary variable identifying the active linear piece of piece-wise affine input−output relation
T = number of time slices
$z_{k,t}$ = binary variable identifying the active linear piece of piece-wise affine input−input relation
α_i = parameter 1 of piece-wise affine input−output relation
βi = parameter 2 of piece-wise affine input−output relation
γ_k = parameter 1 of piece-wise affine input−input relation
δ_k = parameter 1 of piece-wise affine input−input relation
$\eta_{\mathrm{el,\,th}}$ = efficiency of ohmic heating
Θ_t = ambient air conditions (temperature and humidity)

■ INDICES

i = index of piece on piecewise defined input-output relation
k = index of piece on piecewise defined input−input relation
t = time slice index

■ REFERENCES

(1) Rogelj, J.; Shindell, D.; Jiang, K.; Fifita, S.; Forster, P.; Ginzburg, V.; Handa, C.; Kheshgi, H.; Kobayashi, S.; Kriegler, E.; Mundaca, L.; Séférian, R.; IPCC, M. V. *Special Report Global Warming of 1.5 °C*; IPCC, 2018; p 82pp.

(2) *AR6 Climate Change 2021: The Physical Science Basis*; IPCC, 2021; 1−7.

(3) Marcucci, A.; Kypreos, S.; Panos, E. The road to achieving the long-term Paris targets: energy transition and the role of direct air capture. *Climatic Change* **2017**, *144*, 181−193.

(4) Beuttler, C.; Charles, L.; Wurzbacher, J. The Role of Direct Air Capture in Mitigation of Anthropogenic Greenhouse Gas Emissions. *Frontiers in Climate* **2019**, *1*, 3.

(5) Lackner, K. S. Capture of carbon dioxide from ambient air. *European Physical Journal: Special Topics* **2009**, *176*, 93−106.

(6) Minx, J. C.; et al. Negative emissions−Part 1: Research landscape and synthesis. *Environmental Research Letters* **2018**, *13*, 063001.

(7) Meckling, J.; Biber, E. A policy roadmap for negative emissions using direct air capture. *Nat. Commun.* **2021**, *12*, 1−6.
(8) Fuss, S.; et al. Negative emissions - Part 2: Costs, potentials and side effects. *Environmental Research Letters* **2018**, *13*, 63002.
(9) Keith, D. W.; Holmes, G.; St. Angelo, D.; Heidel, K. A Process for Capturing CO2 from the Atmosphere. *Joule* **2018**, *2*, 1573−1594.
(10) Sabatino, F.; Grimm, A.; Gallucci, F.; van Sint Annaland, M.; Kramer, G. J.; Gazzani, M. A comparative energy and costs assessment and optimization for direct air capture technologies. *Joule* **2021**, *5*, 2047−2076.
(11) Fasihi, M.; Efimova, O.; Breyer, C. Techno-economic assessment of CO 2 direct air capture plants. *Journal of Cleaner Production* **2019**, *224*, 957−980.
(12) Sinha, A.; Darunte, L. A.; Jones, C. W.; Realff, M. J.; Kawajiri, Y. Systems Design and Economic Analysis of Direct Air Capture of CO2 through Temperature Vacuum Swing Adsorption Using MIL-101(Cr)-PEI-800 and mmen-Mg2(dobpdc) MOF Adsorbents. *Ind. Eng. Chem. Res.* **2017**, *56*, 750−764.
(13) Azarabadi, H.; Lackner, K. S. A sorbent-focused techno-economic analysis of direct air capture. *Applied Energy* **2019**, *250*, 959−975.
(14) Kong, F.; Rim, G.; Song, M. G.; Rosu, C.; Priyadarshini, P.; Lively, R. P.; Realff, M. J.; Jones, C. W. Research needs targeting direct air capture of carbon dioxide: Material & process performance characteristics under realistic environmental conditions. *Korean Journal of Chemical Engineering* **2022**, *39*, 1−19.
(15) Chen, C.; Tavoni, M. Direct air capture of CO2 and climate stabilization: A model based assessment. *Climatic Change* **2013**, *118*, 59−72.
(16) Hanna, R.; Abdulla, A.; Xu, Y.; Victor, D. G. Emergency deployment of direct air capture as a response to the climate crisis. *Nat. Commun.* **2021**, *12*, 1−13.
(17) Realmonte, G.; Drouet, L.; Gambhir, A.; Glynn, J.; Hawkes, A.; Köberle, A. C.; Tavoni, M. An inter-model assessment of the role of direct air capture in deep mitigation pathways. *Nat. Commun.* **2019**, *10*, 1−12.
(18) Choi, S.; Drese, J. H.; Eisenberger, P. M.; Jones, C. W. Application of Amine-Tethered Solid Sorbents for Direct CO 2 Capture from the Ambient Air. *Environ. Sci. Technol.* **2011**, *45*, 2420−2427.
(19) Elfving, J.; Bajamundi, C.; Kauppinen, J. Characterization and Performance of Direct Air Capture Sorbent. *Energy Procedia* **2017**, *114*, 6087−6101.
(20) Elfving, J.; Bajamundi, C.; Kauppinen, J.; Sainio, T. Modelling of equilibrium working capacity of PSA, TSA and TVSA processes for CO2 adsorption under direct air capture conditions. *Journal of CO2 Utilization* **2017**, *22*, 270−277.
(21) Goeppert, A.; Czaun, M.; May, R. B.; Prakash, G. K. S.; Olah, G. A.; Narayanan, S. R. Carbon dioxide capture from the air using a polyamine based regenerable solid adsorbent. *J. Am. Chem. Soc.* **2011**, *133*, 20164−20167.
(22) Hou, C.; Wu, Y.; Wang, T.; Wang, X.; Gao, X. Preparation of Quaternized Bamboo Cellulose and Its Implication in Direct Air Capture of CO 2. *Energy Fuels* **2019**, *33*, 1745−1752.
(23) Kwon, H. T.; Sakwa-Novak, M. A.; Pang, S. H.; Sujan, A. R.; Ping, E. W.; Jones, C. W. Aminopolymer-Impregnated Hierarchical Silica Structures: Unexpected Equivalent CO2 Uptake under Simulated Air Capture and Flue Gas Capture Conditions. *Chem. Mater.* **2019**, *31*, 5229−5237.
(24) Sanz-Pérez, E. S.; Murdock, C. R.; Didas, S. A.; Jones, C. W. Direct Capture of CO2 from Ambient Air. *Chem. Rev.* **2016**, *116*, 11840−11876.
(25) Sehaqui, H.; Gálvez, M. E.; Becatinni, V.; cheng Ng, Y.; Steinfeld, A.; Zimmermann, T.; Tingaut, P. Fast and Reversible Direct CO 2 Capture from Air onto All-Polymer Nanofibrillated Cellulose-Polyethylenimine Foams. *Environ. Sci. Technol.* **2015**, *49*, 3167−3174.
(26) Sujan, A. R.; Pang, S. H.; Zhu, G.; Jones, C. W.; Lively, R. P. Direct CO 2 Capture from Air using Poly(ethylenimine)-Loaded Polymer/Silica Fiber Sorbents. *ACS Sustainable Chem. Eng.* **2019**, *7*, 5264−5273.
(27) Wurzbacher, J. A.; Gebald, C.; Brunner, S.; Steinfeld, A. Heat and mass transfer of temperature-vacuum swing desorption for CO2 capture from air. *Chemical Engineering Journal* **2016**, *283*, 1329−1338.
(28) Rim, G.; Kong, F.; Song, M.; Rosu, C.; Priyadarshini, P.; Lively, R. P.; Jones, C. W. Sub-Ambient Temperature Direct Air Capture of CO2 using Amine-Impregnated MIL-101(Cr) Enables Ambient Temperature CO2 Recovery. *JACS Au* **2022**, *2*, 380−393.
(29) Deutz, S.; Bardow, A. Life-cycle assessment of an industrial direct air capture process based on temperature-vacuum swing adsorption. *Nature Energy* **2021**, *6*, 203−213.
(30) Terlouw, T.; Treyer, K.; Bauer, C.; Mazzotti, M. Life Cycle Assessment of Direct Air Carbon Capture and Storage with Low-Carbon Energy Sources. *Environ. Sci. Technol.* **2021**, *55*, 11397−11411.
(31) Breyer, C.; Fasihi, M.; Aghahosseini, A. Carbon dioxide direct air capture for effective climate change mitigation based on renewable electricity: a new type of energy system sector coupling. *Mitigation and Adaptation Strategies for Global Change* **2020**, *25*, 43−65.
(32) House, K. Z.; Baclig, A. C.; Ranjan, M.; Van Nierop, E. A.; Wilcox, J.; Herzog, H. J. Economic and energetic analysis of capturing CO2from ambient air. *Proc. Natl. Acad. Sci. U.S.A.* **2011**, *108*, 20428−20433.
(33) Erans, M.; Sanz-Pérez, E. S.; Hanak, D. P.; Clulow, Z.; Reiner, D. M.; Mutch, G. A. Direct air capture: process technology, techno-economic and socio-political challenges. *Energy Environ. Sci.* **2022**, *15*, 1360−1405.
(34) Shi, X.; Xiao, H.; Azarabadi, H.; Song, J.; Wu, X.; Chen, X.; Lackner, K. S. Sorbents for the Direct Capture of CO2 from Ambient Air. *Angew. Chem. Int. Ed.* **2020**, *59*, 6984.
(35) Gebald, C.; Wurzbacher, J. A.; Borgschulte, A.; Zimmermann, T.; Steinfeld, A. Single-component and binary CO2 and H2O adsorption of amine-functionalized cellulose. *Environ. Sci. Technol.* **2014**, *48*, 2497−2504.
(36) Wurzbacher, J. A.; Gebald, C.; Piatkowski, N.; Steinfeld, A. Concurrent separation of CO2 and H2O from air by a temperature-vacuum swing adsorption/desorption cycle. *Environ. Sci. Technol.* **2012**, *46*, 9191−9198.
(37) Joss, L.; Gazzani, M.; Mazzotti, M. Rational design of temperature swing adsorption cycles for post-combustion CO2 capture. *Chem. Eng. Sci.* **2017**, *158*, 381−394.
(38) Streb, A.; Hefti, M.; Gazzani, M.; Mazzotti, M. Novel Adsorption Process for Co-Production of Hydrogen and CO2 from a Multi-component Stream. *Ind. Eng. Chem. Res.* **2019**, *58*, 17489−17506.
(39) Casas, N.; Schell, J.; Blom, R.; Mazzotti, M. MOF and UiO-67/MCM-41 adsorbents for pre-combustion CO2 capture by PSA: Breakthrough experiments and process design. *Sep. Purif. Technol.* **2013**, *112*, 34−48.
(40) Joss, L.; Gazzani, M.; Hefti, M.; Marx, D.; Mazzotti, M. Temperature swing adsorption for the recovery of the heavy component: An equilibrium-based shortcut model. *Ind. Eng. Chem. Res.* **2015**, *54*, 3027−3038.
(41) Marx, D.; Joss, L.; Hefti, M.; Mazzotti, M. Temperature Swing Adsorption for Postcombustion CO2 Capture: Single- and Multi-column Experiments and Simulations. *Ind. Eng. Chem. Res.* **2016**, *55*, 1401−1412.
(42) Joss, L.; Capra, F.; Gazzani, M.; Mazzotti, M.; Martelli, E. *Comput.-Aided Chem. Eng.*; Elsevier, 2016; Vol. *38*; pp 1467−1472.
(43) Drechsler, C.; Agar, D. W. Investigation of water co-adsorption on the energy balance of solid sorbent based direct air capture processes. *Energy* **2020**, *192*, 116587.
(44) *Shipping CO_2 - UK Cost Estimation Study*; Elementenergy, 2018.
(45) OECD. Environment at a Glance 2015. *OECD Indicators* **2015**.
(46) Gabrielli, P.; Gazzani, M.; Martelli, E.; Mazzotti, M. Optimal design of multi-energy systems with seasonal storage. *Applied Energy* **2018**, *219*, 408−424.
(47) Weimann, L.; Gabrielli, P.; Boldrini, A.; Kramer, G. J.; Gazzani, M. Optimal hydrogen production in a wind-dominated zero-emission energy system. *Advances in Applied Energy* **2021**, *3*, 100032.

https://doi.org/10.1021/acs.iecr.2c00681
Ind. Eng. Chem. Res. 2022, 61, 12649−12667

(48) Glover, F. Improved Linear Integer Programming Formulations of Nonlinear Integer Problems. *Management Science* **1975**, *22*, 455−460.

https://doi.org/10.1021/acs.iecr.2c00681
Ind. Eng. Chem. Res. 2022, 61, 12649−12667